COMPARISON OF PARTICLE NUMBER AND MASS EMISSIONS FROM DIESEL TRANSIT BUSES ACROSS TEMPORAL AND SPATIAL SCALES

FINAL REPORT

September 11th Memorial PhD Fellowship sponsored by the New York Metropolitan Transportation Council and the University Transportation Research Center

Darrell B. Sonntag
Fellowship Recipient
Cornell University

Advisors:
H. Oliver Gao, Academic Advisor
Cornell University

Larry McAuliffe, Professional Advisor
NYMTC

EXECUTIVE SUMMARY

Background. Diesel particulate matter (PM) emissions have been estimated to cause more negative health impacts and premature deaths in New York City than any other US city (Clean Air Task Force, 2005). Heavy-duty diesel vehicles emit roughly 10 times the number of particles as gasoline passenger cars (Morawska et al., 2008), and contribute to extremely high ultra-fine particle concentrations near major roadways (McCarthy et al., 2006). Environmental justice concerns are raised because minority and low-income populations are more likely to live in urban areas with high levels of motor vehicle traffic (National Research Council, 2004). In NYC, diesel truck traffic on major freeways and Hunts Point Market is believed to be one of the major reasons the Bronx has the highest asthma mortality rates of the five NYC boroughs (New York City Department of Health, 2003, Lena et al. 2002).

To combat particulate pollution in the region, NYC has taken serious actions to reduce particulate pollution from diesel sources. Through the Clean Fuel Bus Program, the MTA has purchased the largest hybrid-diesel electric bus fleet in the world (1,171 buses), and by the end of 2007, had retrofitted all of the conventional diesel transit buses with diesel particle filters (3,200 buses) (New York City Transit and the Environment). NYC is now focusing on retrofitting heavy-duty diesel vehicles from private fleets (PLANYC 2030).

The number of diesel particles, which are dominated by ultrafine particles (diameter < 100 nm) (Kittelson, 1998), has been proposed as a more effective health measure of PM emissions. Ultrafine particles have the ability to diffuse deep within the lungs and absorb into the bloodstream (Brunekreef and Holgate, 2002) and can contain higher air toxics per unit mass than larger particles (Sioutas et al. 2005). Currently all ambient regulations, tail-pipe emission standards, and regulatory emission models quantify PM according to mass-based metrics (McCarthy et al. 2006). To better address the health risks posed by diesel traffic within the NYMTC region, we propose that we need to also analyze particle number emissions.

Methodology. To better understand the factors that influence diesel particle emissions, particle number emissions were analyzed from a study that collected emissions in real-world driving conditions in Hartford, CT area. The study measured particle number emissions from both conventional diesel and hybrid buses under two types of retrofit technologies considered by PLANYC: diesel oxidation catalysts (DOC) and diesel particle filters (DPF) (PLANYC 2030).

The collected emissions data was time-aligned to engine operating parameters, and plotted on the road network using Geographical Information Systems (GIS). Particle mass emissions were plotted alongside particle number emissions to determine if high-emitting events of both PM metrics occurred in the same locations on the road network. The size-distribution of the particle emissions was also evaluated in order to understand the relationship among the two metrics. General relationships between particle emissions and operating parameters were estimated using statistical models. In addition, ratios between number and $PM_{2.5}$ emissions were estimated according to different operating modes and roadway conditions. By understanding these relationships, air quality analysts and planners can better estimate ultrafine particle emissions, when limited data is available to estimate emissions.

Findings Relative to Air Quality Management Goals of the NYMTC Region.

Summary Table. Particle number and mass emission rates for evaluated data. (Refer to qualifications on page 3, before making conclusions using the reported data)

Roadtype/ Opertating Mode	Number, 10^{12} particles/s	Mass, mg/s	Number, 10^{12} particles/g fuel	Mass, mg particles/g fuel burned	Number, 10^{12} particles/mg mass of particles emitted
Urban Arterial	**172**	**19.7**	**0.6**	**0.07**	**8.7**
Acceleration	295	32.8	0.6	0.07	9.0
Deceleration	52	5.3	0.7	0.07	9.8
Idle	NA	NA	0.4	0.13	3.1
Cruise	89	6.6	0.6	0.05	13.5
Rural Arterial	**123**	**18.8**	**0.5**	**0.08**	**6.5**
Acceleration	406	50.7	0.7	0.09	8.0
Deceleration	9	2.3	0.2	0.05	4.1
Idle	NA	NA	0.6	0.16	3.8
Uphill Cruise	253	47.7	0.5	0.10	5.3
Downhill cruise	36	2.8	0.5	0.04	13.1
Level cruise	71	6.1	0.7	0.06	11.6
Divided Freeway	**268**	**38.05**	**1.0**	**0.15**	**7.0**
On Ramp	243	47.5	0.5	0.10	5.1
Off Ramp	37	4.5	0.4	0.05	8.3
Acceleration	248	36.3	0.7	0.10	6.8
Deceleration	105	10.9	1.1	0.12	9.7
Cruise	282	39.9	1.1	0.15	7.1
Overall	**211**	**29.03**	**0.8**	**0.11**	**7.3**

Conclusions made from buses with equipped with Diesel Oxidation Catalysts

- Number and mass emission rates are highly correlated across the road network.
- High-emitting episodes of PM mass emissions coincided with high-emitting episodes of particle number emissions
- Focusing efforts on reducing the hot-spots identified from PM mass measurements should also reduce particle number emissions.
- Both time-based and distance-based emission rates should be considered in evaluating transportation emissions. For example, the locations on the road network that where the bus emitted the most emissions/km were not the episodes that had the highest emission/second rates.
- The largest emitting episodes occurred at bus stops and intersections where the bus was accelerating from stop. By removing excessive stop-and-go traffic, traffic engineers and urban planners can improve air quality.
- Even though the largest episodes of high emissions occurred on the urban arterial, on average, the particle mass and number emission rates were substantially higher on the freeway compared to the urban arterials. Thus, the urban route had more variable emissions, while the freeway has more constant, but higher, emissions.

- Idling contributed little to particle mass or particle number emissions, unless the bus was extended idling (more than several minutes). Cold-start idling also did not significantly increase particle number emissions. However, DPF-equipped buses likely have elevated idling emission rates after cold-starts (Mathis, et al. 2005).
- Number and mass emission rates were repeatable functions of engine operating conditions and roadway type. Similar observations were observed across two days of testing in real-world driving conditions.
- Because number and mass emissions are highly correlated for the DOC-equipped buses, the ratio: *particle number*/*particle mass* could potentially be used to estimate particle number emission rates when only mass emission rates are provided by emission models (i.e. EPA's MOVES). *Particle number*/*Particle mass* ratios were computed for the summary Table on page 2. However, future research is needed to estimate the ratios on a broader sample size of vehicle types.
- Particle mass and number are both well correlated with fuel rate. Using *Particle number*/*fuel* and *particle mass*/*fuel* ratios are reasonable approaches to estimate emissions using limited data.
- To limit particle exposure, the NYMTC could implement several practices.
    1. By eliminating unnecessary accelerations (through priority intersections or exclusive bus lanes), DOC-equipped diesel vehicles could significantly reduce particle exposure in terms of number and mass.
    2. While acceleration events dominate emissions for typical stops, idling can be significant if the vehicle idles for several minutes. Enforcement of anti-idling policies can have a significant benefit on both particle number and mass emissions.
    3. The cleanest vehicles should be used on the routes that have the highest population exposure and the highest distance-based emission rates. We would recommend using the cleanest vehicles be used on the urban arterials, because of the close proximity of pedestrians and urban residents to the roadway. The divided freeways typically have larger shoulder, allowing more time and distance for high particle number concentrations to decay before reaching populated areas offset from the freeway.

Conclusions made from the buses with equipped with Diesel Particle Filters

- Particle mass emissions are significantly reduced by diesel particle filters as confirmed in many studies (over 95%).
- Data is inconclusive about effect of operating mode or the effect of hybrid buses on particle emissions
    - The drop in emissions with hybrid appears to be solely due to the diesel particle filters, not hybrid technology (Sonntag et al. 2008).
    - Due to low resolution at low emission concentrations, the effect of operating mode cannot be quantified. More discussion is included on pages 25-26.

Qualifications of data

- The data was collected under the state of the practice techniques, however the difficulty of measuring particle number emissions in real-operating conditions may have suppressed the formation of a very large nucleation mode that is present in real-world exhaust from both conventional diesel vehicles (page 17) and diesel vehicles with diesel particle filters (page 25).
- The particle mass emission rates measured in our study from the DOC-equipped buses are significantly lower than emission rates reported in the literature (see page 17), and better correspond to emission rates for buses equipped for DPF buses in other studies. Because the number and mass emission rates are consistent with one another (pages 24-25), we believe the systematic lower emission rates is due to an incorrect dilution ratio (page 17).
- Similarly, the measured particle emission rates for the DPF-equipped buses are roughly 10 times smaller than emission rates reported for similar studies of DPF-equipped buses. Again, most of the error is believed to be due to an incorrectly measured dilution ratio. Additional error is also introduced due to difficulties in calculating both number and mass emissions from DPF-equipped buses, and the incorrect (page 25-26).
- While the absolute magnitude of particle number and mass emissions may not be valid, the relative variation of the particle number and mass emissions rates are believed to be valid for the qualifications given (pages 17-18). The size distribution of particles is similar to previous studies conducted using artificial dilution tunnels (page 18). Repeatable observations are obtained from testing on different days on the same routes (page 15).
- There was large decrease in particle number emissions observed due to the implementation of diesel particle filters. However, the most recent studies of diesel particle filters have shown that the number of particles can increase with the use of diesel particle filters, due to the increased formation of volatile sulfate-derived nanoparticles. However, particle mass and solid particle number will largely be decreased with diesel particle filters. Additional details are discussed on page 25.

Future Research

- Better measurement protocols and sampling systems are needed to accurately measure the number and mass emission rates from buses with low vehicle emissions, including the NYC DPF-equipped buses.
- Current measurement techniques have the potential to accurately measured particle mass emission rates for conventional diesel vehicles. However, future work is needed to accurately measure the number concentrations of particles below 30 nm, in real-operating conditions. The current state-of-the art particle sampling practices often suppress the formation of volatile nucleation mode particles that are observed in real-world exhaust plumes.
- Particle number concentrations can be measured at PM hot-spots, such as the Hunts Point Market, to better evaluate the risk of diesel particle emissions.
- More comparisons need to be made with additional vehicle types to confirm that mass and number emission rates are well correlated under different vehicle types, fuels, aftertreatments, sampling conditions and driving conditions.

FULL REPORT

COMPARISON OF PARTICLE NUMBER AND MASS EMISSIONS FROM A DIESEL TRANSIT BUS ACROSS TEMPORAL AND SPATIAL SCALES

Darrell B. Sonntag, H. Oliver Gao, and Britt A. Holmén

Abstract

Two common metrics of particle pollution measure the total number of particles (particle number) and the total mass of the particles (particle mass). This work analyzes particle number and mass emission rates measured from the exhaust of a 2002 diesel transit bus in real-driving conditions using on on-board mini-dilution system. The number concentrations were measured using the Electrical Low Pressure Impactor (ELPI) across a particle range of 7 to 10,060 nm, with 93% of the total particle number concentration measured below 95 nm. Mass emission rates were derived from the number counts using the bottom stages of the ELPI (7 to 387 nm) and were verified to be consistent with concurrent gravimetric filter measurements made on-board the bus. The behavior of the number and mass emission rates are examined at resolved temporal and spatial scales across three facility types: an urban arterial, a rural arterial and a divided freeway. The time-based particle emission rates are highest on the freeway, but at select 50-meter segments the distance-based particle emission rates (i.e., "hot-spots" for exposure assessment) occur at intersections when the bus accelerates from a stop. Generally, the number and mass emissions are highly correlated both temporally and spatially. Some deviations do occur because particle mass emissions are highly elevated during sustained fueling events, such as traveling on high grades and sustained accelerations, while particle number emissions are more sensitive to fuel and engine speed fluctuations. The observations are validated using statistical models across two days of testing. The results should be used with qualification, as the sampling system did not fully measure the nucleation mode concentrations which contain the majority of the particle numbers in diesel exhaust. The size distribution data are consistent with heavy-duty vehicle emission sampled from artificial dilution tunnels. However, much higher nucleation mode concentrations were detected from studies that 1. Sampled particles directly from the exhaust plume, and 2. Accurately measured particles with diameters smaller than 7 nm.

Introduction

Single metrics are used to represent the entire distribution of particulate matter (PM) emitted from vehicle exhaust. Two common metrics evaluate the total number of particles (particle number) and the total mass of the particles (particle mass). For diesel exhaust from conventional heavy-duty vehicles, ultrafine particles (<100 nm) dominate the total number emissions, but contribute little to the total mass of the diesel particles (Kittelson et al., 2004). Fine particles (< 2.5 um) from heavy-duty diesel vehicles contain the majority of mass, with the peak in particle mass distribution occurring between 100 and 180 nm for heavy-duty diesel vehicles (Robert et al., 2007).

Both metrics are useful from a health perspective, however the relative importance of each are not readily understood. Currently all U.S. ambient regulations, tail-pipe emission standards, and regulatory emission models quantify PM according to mass-based metrics (McCarthy et al., 2006). The number of diesel particles has been proposed as a more effective health measurement of PM emissions because ultrafine particles have the ability to diffuse deep within the lungs and absorb into the bloodstream (Brunekreef and Holgate, 2002) and can contain higher air toxics per unit mass than fine particles (Sioutas et al. 2005).

The spatial distribution of ambient particle concentrations differs significantly depending on the particle size. Near major roadways, particle number concentrations can be more than ~25

times higher than background levels, while mass-based metrics such as $PM_{2.5}$ are only slightly elevated (Zhu et al., 2002). These spatial differences have caused researchers to suggest that ultrafine particles may play a key role in the increased risk of mortality and children asthma observed near major roadways (Brunekreef and Holgate, 2002; American Lung Association, 2007). To better understand the relative health effects of ultrafine particles and fine particles, more data is needed on their spatial distribution in urban areas (Wichmann and Peters, 2000).

Number and mass-based particle emission measurements from different heavy-duty diesel vehicles do not necessarily correlate (Kittelson, 1998). Limited work has been done that examines the correlation of vehicle-specific number and mass emission rates during vehicle operation. Stationary roadside measurements of total particle number concentrations (> 7 nm) and particle volumes (18 to 300 nm) which is often a surrogate for particle mass) have shown positive correlation through the day due to changing traffic conditions (Imhof et al., 2005). Aerosol transformations that occur after particles exit the tailpipe, as well as background particle concentrations, lead to substantially different temporal distributions of PM1 or PM10 at the same sampling location (Imhof et al., 2005). While the majority of the temporal and spatial differences in the distribution of mass and number measurements are most likely due to post-emission processes, it is worthwhile to examine the variation of particle mass and number emissions due to changing vehicle operating conditions.

This work examined particle number and mass emissions measured from the tailpipe of a diesel transit bus traveling through a real-world road network. By measuring emissions using on-board artificial dilution conditions, the study is somewhat of a cross between a stationary dynamometer study and an on-road ambient measurement study. Stationary dynamometer studies are vital for establishing relationships between vehicle operation and particle emissions in controlled environments (Robert et al. 2007, Kittelson et al., 2006a). Two aspects make on-board emissions data unique from dynamometer studies, 1. Emissions are spatially allocated in the road network, and 2. Real-world driving conditions are sampled that cannot be fully replicated on a chassis or engine dynamometer (Kittelson et al., 2006a, Robert et al., 2007).

Vehicle chase and road-side measurements are vital for quantifying the nature of particles that people are exposed to on and near roadways. Two aspects set this study apart from ambient studies. 1. By measuring the emissions of one vehicle using an artificial dilution system, the study side-steps the confounding effects of other vehicle emissions, background concentrations, and transformation processes that can change dramatically on different days. 2. Continuous high-resolution data can be collected from the bus under all driving conditions, as compared to chase-studies that collect intermittent data over average driving conditions.

The objective of this study is to understand the behavior of particle mass and number emissions from a diesel transit bus across time and space in a real-transportation network. The particle number emission rates from the evaluated bus have been analyzed previously (Vikara and Holmen, 2006, chapter 2 and 3, Jackson and Holmen, 2009). However, temporally and spatially-resolved mass-emission rates were not previously computed or analyzed. This study specifically compares the effect of operating modes and road network conditions on particle number and mass emissions.

Experimental

The analyzed emissions data was collected by Holmén et al. (2005) on four Connecticut Transit buses in 2004. In this work, data from one bus collected over a two-day period was analyzed in detail. The 2002 model year transit bus was equipped with a direct injection, turbocharged Detroit Diesel Series 40 engine, with a diesel oxidation catalyst (DOC). The bus was tested on September 20th and 21st under multiple driving conditions common to bus routes in the Hartford, CT area, including a high-speed divided freeway, stop-and-go urban arterial, and rural arterial with sections of high-grade (Table 5.1). The daily test was conducted along three routes, each of which was tested with an out-bound and an in-bound run. After each route was tested (typically 18-30 minutes), a Teflon-coated glass fiber filter was removed and subsequently post-weighted to calculate the particle mass concentration.

The PM size distribution of the diesel exhaust was measured on-board the bus using a TSI, Inc. Scanning Mobility Particle Sizer (SMPS) and a Dekati, Ltd. Electrical Low Pressure Impactor (ELPI) connected to a partial flow, single-stage mini-dilution system. The exhaust sample flow was divided into two parallel mini-diluters, from the first mini-diluter, the SMPS and ELPI measured the particle-size concentration, and from the second mini-diluter the gravimetric filter collected the particle mass emissions.

The ELPI measures real-time particle number concentration using 12 size cuts according to aerodynamic diameter between 30 nm and 10,000 nm. The ELPI was equipped with the electrical filter stage which extends the measurable range of particles down to 7 nm. The SMPS was operating on size-selective mode, and cannot measure the entire particle size distribution at a high temporal resolution, whereas the ELPI particle number measured the particle number concentrations the 12 impactor stages every 1~2 seconds. The SMPS and ELPI measurements from the study were previously shown to coincide (Holmén et al., 2005). The purpose of this work was focused on the effect of transient vehicle behavior on particle emissions, so only the real-time ELPI measurements were analyzed in this study.

The on-board instrumentation included a Horiba OBS-1000 gas emission analyzer, which measured fuel rate, gaseous emissions (NOx, CO_2, CO, HC), and the exhaust flow rate using a calibrated pitot tube. The exhaust flow rate was corrected for negative and unreasonably low readings by assuming a minimum exhaust flow of 1300 L/min (See Supporting Information). A global positioning system unit on the Horiba OBS-1000 was used to spatially locate the bus on the defined bus routes, for which accurate grade data was available. A data link adapter connected to the network port of the diesel bus recorded instantaneous engine operation data. Further information on the measurement equipment, bus specifications, and experimental design is detailed in the report by Holmén et al. (2005).

Time-based Particle Emission Rates. The size-distributed particle number measurements from the ELPI and the exhaust flow measurements from the Horiba were time aligned with the engine operation parameters to account for the residence and transport time of emissions in the exhaust and dilution system. A constant lag was applied that maximized the cross-correlation between the ELPI, Horiba and engine parameters. Once all the data was synchronized to the engine data, the particle number emissions rate was calculated by multiplying the particle number concentration, total exhaust flow rate (Q_T) and dilution ratio (DR) for the runs on September 20th and 21st:

$$Particle\ Number\ Emission\ Rate\left(\frac{\#}{\sec}\right) = Particle\ Number\ Concentration \times Q_T \times DR$$

The average dilution ratio was 31 and 29 for September 20th and 21st, respectively.

Time-resolved mass emission rates were calculated using the ELPI measurements. Only particle counts on the electrical filter stage and lower five stages of the ELPI were used

(diameters < 387 nm), assuming unit-density spherical particles with diameters equal to the geometric mean of the respective impactor stages, as done previously by Kinsey et al. (2006). The large diameter particle readings from the upper stages were excluded because positive artifacts on the upper stages can greatly affect mass concentration estimates (Maricq et al., 2006).

The ELPI-derived mass concentrations were compared to the route-level filter mass measurements. For the 12 test runs conducted on September 20th and 21st, the ELPI-derived PM mass concentrations were 14% larger than the route-level, filter-based PM mass concentrations and were positively correlated with a R^2 =95%. The lower-stage measurements of the ELPI therefore appear to be a usable surrogate of the total PM mass emissions, and suggest that the accumulation mode measured by the ELPI (56.4- 387 nm) contained the majority of the particle mass. A time-resolved PM mass emission rate was subsequently computed from the ELPI-derived mass concentrations using the exhaust flow rate and dilution ratio as was done in equation (1). Table 5.1 displays the mean particle number and mass emission rates according to facility types and operating modes.

Table 5.1. Summary of Particle Emission Rates for September 20th NE Runs analyzed by Road Type and Operating Mode.

	Descriptive Statistics, Time-based means					Time-based emission rates		Distance-based emission rates		R^2 between number and mass emissions (time-based)
Roadtype/ Opertating Mode	Time, sec	Speed, kph	Accel, kph/s	Grade, %	Fuel, g/s	Number, 10^{12} particles/s	Mass, mg/s	Number, 10^{12} particles/km	Mass, mg/km	
Urban Arterial	**2362**	**19**	**0.0**	**-0.4**	**1.5**	**0.9**	**0.11**	**172**	**20**	**0.81**
Acceleration	801	23.8	1.9	-0.5	3.2	1.9	0.22	295	33	
Deceleration	690	20.8	-2.2	-0.6	0.5	0.3	0.03	52	5	
Idle	629	0.0	0.0	-0.2	0.4	0.2	0.05	NA	NA	
Cruise	242	50.3	0.0	-0.3	2.0	1.2	0.09	89	7	
Rural Arterial	**736**	**49**	**0.0**	**-0.2**	**3.1**	**1.7**	**0.26**	**123**	**19**	**0.62**
Acceleration	63	26	2.6	-1.9	4.1	2.9	0.37	406	51	
Deceleration	61	20	-2.7	-1.3	0.2	0.1	0.01	9	2	
Idle	31	0	0.0	0.6	0.3	0.2	0.04	NA	NA	
Uphill Cruise	203	53	0.0	5.6	7.3	3.7	0.70	253	48	
Downhill cruise	266	61	0.2	-4.1	1.1	0.6	0.05	36	3	
Level cruise	112	58	-0.4	-0.1	1.8	1.2	0.10	71	6	
Divided Freeway	**932**	**95**	**0.02**	**0.0**	**6.8**	**7.0**	**1.00**	**268**	**38**	**0.54**
On Ramp	32	56	1.9	NA	7.4	3.8	0.74	243	47	
Off Ramp	33	49	-0.9	-0.7	1.3	0.5	0.06	37	4	
Acceleration	25	90	1.3	-1.1	8.6	6.2	0.90	248	36	
Deceleration	41	90	-1.9	0.4	2.4	2.6	0.27	105	11	
Cruise	801	98	0.0	0.0	7.2	7.7	1.09	282	40	
Overall	**4030**	**42.2**	**0.01**	**-0.3**	**3.0**	**2.5**	**0.34**	**211**	**29**	**0.80**

Distance-based Particle Emission Rates. Air quality models require spatially allocated emission factors along a roadway or a grid (Zhang et al., 2005). Distance-based emission rates (emissions per kilometer), are used to spatially allocate emissions and are important for estimating pollution exposure from emissions for persons on or near the road network. Average distance-based emission rates were calculated by dividing the average time-based emission rates

for each operating mode by the average speed, yielding emissions per kilometer in Table 5.1. Idling emission rates cannot be expressed or calculated in per-distance terms, although the emissions from idling are included in the mean emission rates at the facility type level. Table 5.1 is discussed in more detail in the exploratory analysis.

Exploratory Analysis

Across the entire dataset, the particle number and mass metrics are well correlated across time (R^2 =.80 from Table 5.1), due in part to the overall variability between high and low load vehicle operation. Within given roadway types or operating modes, such as on the divided freeway, the linear correlation is considerably less. To better understand the behavior of each metric on each roadway type, the particle emission rates were evaluated in detail for 3-minute periods from each of the three dominant facilities (Figures 1, 2, and 3). Each 3-minute period was chosen such that it demonstrated the unique driving conditions of each facility. During the urban arterial, the three minute segment included a section of roadway where the bus stopped four times within 800 meters. The 3-minute section for the rural arterial included an extensive high-grade section with the grade averaging 6.2% for over 2.2 kilometers, with the maximum grade exceeding 9%. On the selected freeway segment, the bus traveled 5.4 kilometers at an average speed of 102 km/hr. Time-series profiles of the time-based particle measurements, and two engine covariates, fuel rate and engine speed, were plotted for each dominant roadway type (Figure 5.1,5.2 and 5.3).

Distance-based PM emission rates were aggregated in terms of number and micrograms per kilometer for every 50, 100, and 200 meter segment for the urban arterial, rural arterial and divided freeway, respectively. By spatially aggregating, the idling emissions were accounted for in each interval, and the particle exposure of the bus can be better interpreted using Geographical Information System (GIS) plots. The GIS plots (Figure 5.1-3, 5.2-3, and 5.3-3) provide a "bird's eye view" of the distance-based emissions rates plotted spatially along the testing route for the same 3-minute period analyzed in the time-series plots. Each segment is color coded according to the percentile of emission rates compared to the entire testing route, with the numerical values for each percentile provided in the supporting documents (Table 5.A5). Different levels of spatial aggregations were used (50, 100, and 200 meters) to maximize the spatial resolution, while assuring that each 50, 100 or 200 meter segment contained at least one particle measurement. The particle number emission rates are plotted in parallel above the particle mass emission rates. A corresponding GIS plot (panel 4) provides information on two roadway covariates, the average grade of each segment, and the average speed of the bus.

In Figures 1 through 3, the particle number size-distributions are plotted for the observations that occurred during select episodes. The episodes are defined over 100, 200, or 400 meter intervals according to roadway type. The episodes were chosen at locations along the road network that may potentially be PM "hot-spots" due to relatively high particle number and/or mass emissions. Spline smoothing was used to approximate smooth particle size distributions from the ELPI discrete measurements. Mass-weighted size-distributions are included in the supporting information (Figure 5.A8). Key observations about the emission rates are noted on the figures, while comparisons and discussions are included in the text.

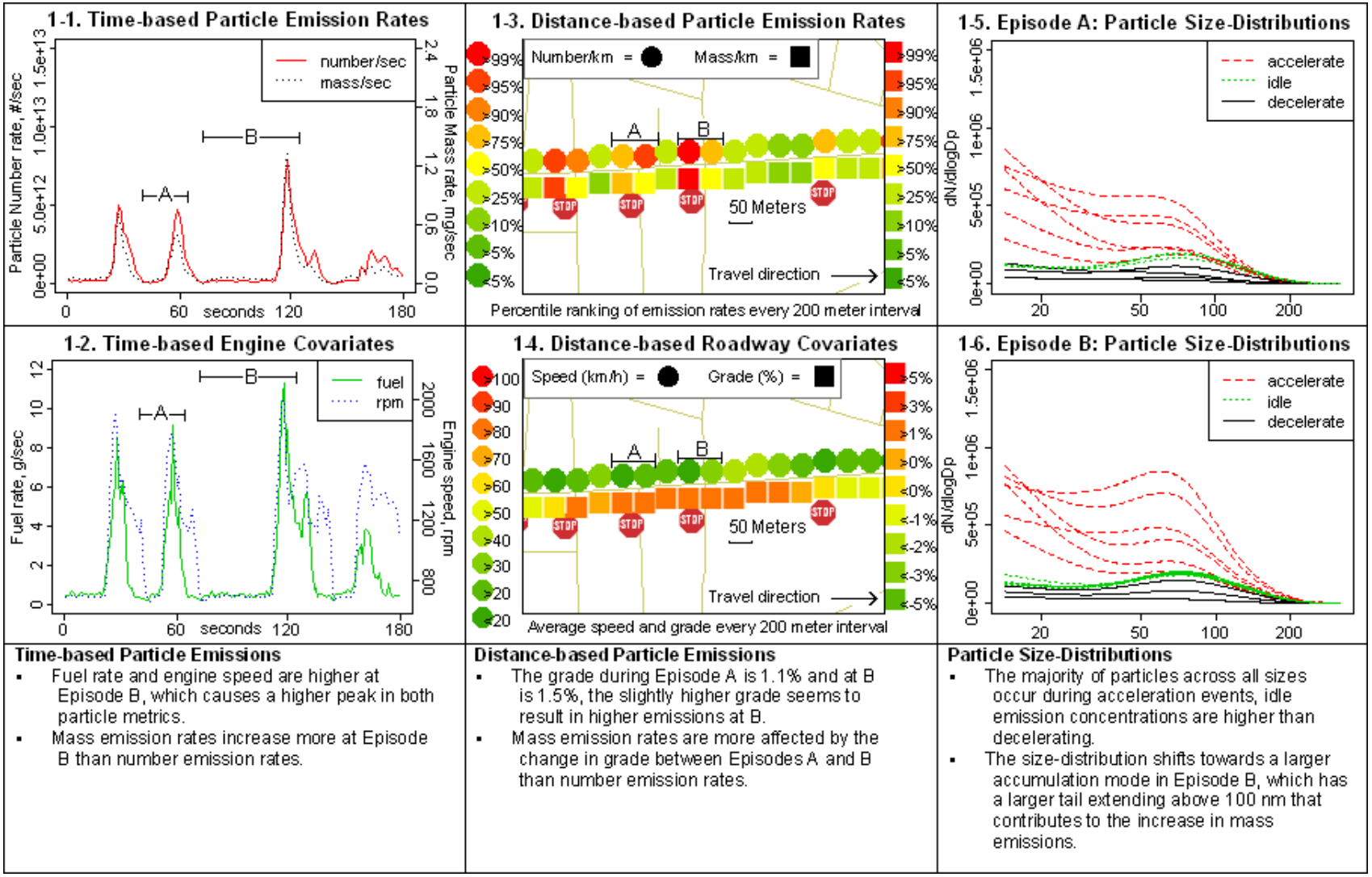

Figure 5.1. Detailed particle number and mass emission rates for a three-minute segment of the urban arterial. Figure 5.1-1: Time-series plot of particle number and mass emission rates. Figure 5.1-2: Time-series plot of fuel rate and engine speed. Figure 5.1-3: GIS plots of distance-based emission rates for every 50 meter segment. Figure 5.1-4: Average grade and speed over 50 meter segments. Figures 1-5 and Figure 5.1-6: Particle number size-distribution concentrations measured for two 100-meter segments (Episodes A and B).

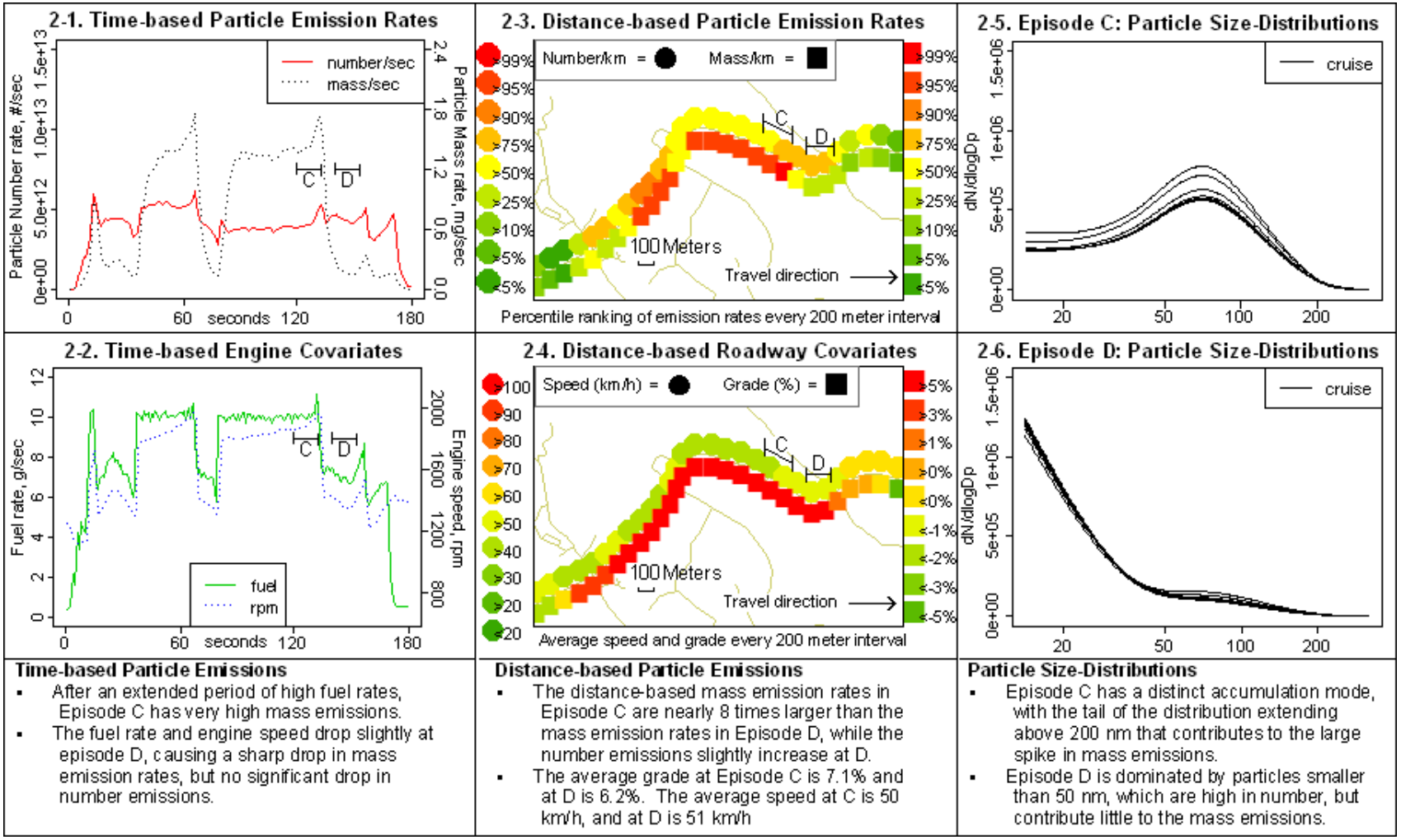

Figure 5.2. Detailed particle number and mass emission rates for a three-minute segment of the rural arterial. Figure 5.2-1: Time-series plots of particle number and mass emission rates. Figure 5.2-2: Time-series plots of fuel rate and engine speed. Figure 5.2-3: GIS plots of distance-based emission rates for every 100 meter segment. Figure 5.2-4: Average grade and speed over 100 meter segments. Figures 2-5 and Figure 5.2-6: Particle number size-distribution concentrations measured for two 200 meter segments (Episodes C and D).

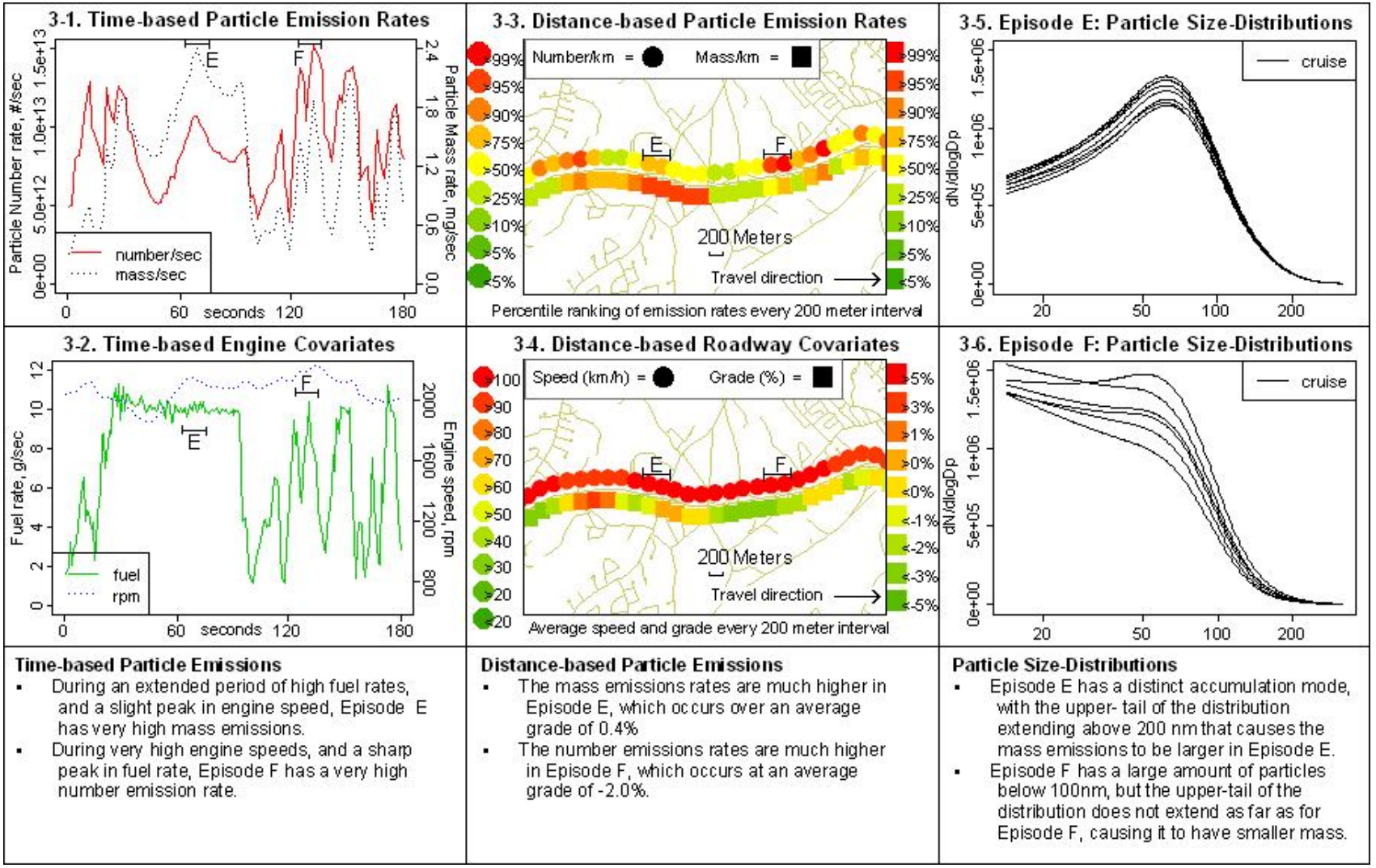

Figure 5.3. Detailed particle number and mass emission rates for a three-minute segment of divided freeway. Figure 5.3-1: Time-series plots of particle number and mass emission rates. Figure 5.3-2: Time-series plots of fuel rate and engine speed. Figure 5.3-3: GIS plots of distance-based emission rates for every 200 meter segment. Figure 5.3-4: Average grade and speed over 200 meter segments. Figures 3-5 and Figure 5.3-6: Particle number size-distribution concentrations measured for two 400 meter segments (Episodes E and F).

Urban Arterial. On the urban arterial, the number and mass emission rates spike as the bus accelerates. Due to the low speed and relative high emission rates during acceleration, large distance-based emission rates occurred near the bus stops and intersections as is evident from Table 5.1 and Figure 5.1-2. By only examining the GIS plot, it may seem reasonable that the elevated emission rates at the intersections could also be due to idling, where the bus was emitting particles but not traveling any distance. Each of the 50-meter segments that captured the 41 stops along the bus route was further evaluated by operating mode (Table 5.A4). The majority of emissions occurred due to acceleration (82.0% of the total particle number emissions and 68.1% of the total particle mass emissions), with the rest split between idling and deceleration. The median idling time was 9 seconds and the median acceleration time was 8 seconds. For the bus to have contributed an equal amount of emissions during idling as accelerating during a typical 50 meter segment, the bus would have to idle for more than 45 seconds (for particle mass) and almost 2 minutes (for particle number). Unless the buses were to idle for an extended stop, particle exposure can be mainly attributed to acceleration events on the stop-and-go arterials.

Rural Uphill. On the uphill accent on the rural arterial, the bus emitted elevated, but relatively stable particle numbers. The mass emissions were highly responsive to the fuel rate and engine speeds, producing variable and very high mass emission rates. The shape of the particle-size distribution varied drastically within the uphill accent (Figure 5.2-5 and 2-6), permitting the number emissions to stay relatively constant, while the mass emissions varied considerably (Figure 5.2-1). For the rural arterial, the distance-based mass emission rates were among the highest on the entire route, while the number emissions were only moderately elevated (Table 5.1).

Divided Freeway. The time-based particle number and mass emission rates reach their maximum values across the entire bus route on the segment of divided freeway in Figure 5.3. Both the particle number and mass emissions are highly variable, as the bus sustains high engine speeds and a large range of engine loads. Number and mass emissions were positively correlated (R^2=0.54), but also behave remarkably different as evidenced by the dynamic behavior of the particle size-distribution. Particle number emissions appear to be more influenced by short spikes in fuel rate, rather than long-sustained segments of high fuel rate.

Although the bus is cruising within a narrow speed window, the distance-based particle emissions do have considerable spatial variation. The high-emitting episodes for particle mass and number appear to occur at or slightly before positive changes in grade. The rural and urban arterials have short segments where the distance-based emission rates are larger than the freeway. However, due to constant high load conditions on the freeway, the average emission rates are highest on the divided freeway for both particle metrics (Table 5.1).

Modeling Section

The observations made from the exploratory analysis were statistically evaluated by modeling the relationship between particle emissions and engine parameters. Individual statistical models were estimated for particle number and mass emissions for three sections of the bus route. The urban section was 23 minutes in length and captured stop-and-go conditions, the rural hill section captured uphill and down hill sections of the rural arterial (6 minutes) and the freeway section captured the entire trip on the freeway including the on-ramp and off-ramp (16 minutes). The time-based emission rates were aggregated every 3-seconds for analysis because the ELPI only recorded particle concentrations every 1-2 seconds, and the standard deviation of the time lag between the engine and the ELPI was estimated to be 2.01 seconds (Holmen et al., 2005).

Linear regression models were estimated with normalized emission rates and engine parameters, $(y-\bar{y})/\sigma_y$, so that the parameters could be more easily compared between the number and mass models, and between different engine parameters. Although non-linear relationships are likely to exist between the particle emissions and engine covariates, by estimating separate models for each roadway condition, linear models were anticipated to be able to approximate this relationship while maintaining interpretability. The linear models were estimated in the following form:

$Particle\ emission\ rate(\ per\ second\ ) = \beta_o + \sum_{i=1}^{k}(\beta_i \cdot engine\ parameter_i) + \varepsilon$, for both the particle number and mass emission rates. Three engine parameters were evaluated for inclusion in each model: fuel rate, engine speed, and exhaust temperature. Previous analysis found that these parameters explained the majority of the engine parameter variation of the dataset (Sonntag, 2009). In addition, transformations and lags of the covariates were also considered to capture the temporal-dependence of the emission rates and approximate non-linear relationships. For example, the marginal effect of fuel rate on particle emissions appears to depend on the level of fuel rate. This non-linear relationship was approximated in the linear model by raising fuel rate to the second power. Each term was included in the model if it was significant at the 5% level on both the September 20th and 21st datasets. If one of the three original engine parameters was not significant but its transformation or lag was significant (i.e. $Fuel^2$) then both terms were included in the model. The estimated model parameters from September 20th are displayed in Table 5.2, and September 21st in Table 5.A7.

Table 5.2. Model Coefficients

	1. Urban Model		2. Rural Hill Model		3. Freeway Model	
Parameter	Number	Mass	Number	Mass	Number	Mass
Intercept	-0.34	-0.44	-0.13	-0.71	-0.04	-0.53
Fuel	0.22	0.22	0.40	0.01	0.32	0.10
$Fuel^2$	0.18	0.32	-0.14	0.21		0.28
$Fuel_{t-1}$	0.26	0.19	0.28	0.25	0.23	0.43
Engine Speed	0.30	0.24		0.48	-0.33	-0.96
$Engine\ Speed^2$	0.12	0.10		0.63	1.19	0.91
$Engine\ Speed_{t-1}$	-0.03	-0.10				
Exhaust Temperature	-0.08			-0.05	-0.70	0.12
Fit Statistics						
Adjusted R^2	0.95	0.93	0.91	0.97	0.86	0.89

Results

Urban Model. As expected, number and mass emissions are both well predicted using fuel and engine speed. The coefficients for the $Fuel^2$ and $EngineSpeed^2$ terms are both positive, meaning their marginal effect on both particle mass and number emissions increases at higher levels. The $Fuel^2$ coefficient is larger for mass emissions, while the $EngineSpeed^2$ coefficient is larger for number emissions. The negative effect of the lagged engine speed (the engine speed 3-seconds prior) likely captured the effect that, during deceleration engine speed can still be high, while emissions are low.

Rural Hill Model. On the rural hill section, particle mass is a stronger function of the operating conditions (R^2=0.97) than particle number emissions (R^2=0.91). Fuel rate and engine speed are significant predictors for mass emissions, but only fuel rate is a significant predictor for number emissions. Mass emissions are increasingly affected by fuel rate and engine speed at higher levels, as evidenced from the positive $Fuel^2$ and $EngineSpeed^2$ coefficients. Interestingly, the $Fuel^2$ coefficient is negative in the number model. As fuel rate increases, the marginal fuel effect on number decreases as it approaches the maximum fuel rate. Exhaust temperature was not significant in the number emission models, but it did have a significant negative effect on the particle mass emissions.

Freeway Model. As was evident from the exploratory analysis, fuel rate has a larger effect on mass emissions, while engine speed has a larger effect on number emissions. Number emissions were not significantly effected by large spikes in fuel rate ($Fuel^2$ coefficient is insignificant); however, the $EngineSpeed^2$ has a large positive effect. Mass emissions are positively influenced by spikes in both fuel and engine speed. Exhaust temperature had a different relationship on particle number and mass emissions. For particle number it was strongly negative, and was moderately positive for particle mass.

Model Verification. The same models were fit for the same sections of roadway tested on September 21, 2004. The models had similar fits to the data both in terms of R^2 values and model coefficients. The model coefficients for all significant variables were of similar magnitude and had the same positive/negative signs (Table 5.A7). Even though the statistical models did not pass all diagnostic tests for normal independently distributed residuals, confirming the results on separate data sets provides robust evidence that the models estimated true relationships between particle emissions and the evaluated engine parameters.

Discussion

The statistical models are useful for comparing the engine factors influencing particle number and mass emissions, rather than quantifying an absolute relationship between particle emissions and engine operation. The model intercepts and coefficients change significantly across facility types, due to the effect of approximating highly non-linear and complex data with simple linear relationships. From these models, conclusions need to be made within "context" or the "facility effect" of each model in consideration. For the estimation of more general relationships between particle number and operating parameters across different driving conditions, see Sonntag and Gao (2009), which estimated particle number emission at the roadway link-level. However, several conclusions about the transient behavior of particle number and mass emissions can be drawn from the observed data and model results:

1. Mass emissions are a strong function of the fuel rate, and are especially sensitive to high fueling rates. All the fuel coefficients, including the $Fuel^2$ coefficient was positive and significant in all three mass emission models. Previous observations confirm that diesel transit bus particulate mass emissions are a strong function of fuel transients (Hofeldt and Chen, 1996). Peaks in mass emission rates occur at high fuel rates regardless of the duration of the engine load. In some instances, it appears the large mass emission rates are favored by sustained fueling events. For example, the largest mass emission rates on the rural and freeway route occur during sustained high-fueling events (Figure 5.2-1 and 3-1).

2. In contrast, particle number emission rates had more complex relationships with the engine parameters coefficient depending on the roadway type. The changing relationships with number emissions appear to be caused by the storage and release of particles from the engine and exhaust system. During the intermittent, hard accelerations on the urban arterial, the particle number emissions are positively associated with both $EngineSpeed^2$ and $Fuel^2$. However, on the

rural hill route, which contains a long uphill section with sustained high loads, $Fuel^2$ has a negative effect on particle number emissions and engine speed was insignificant (Table 5.2). On the freeway route, particle number emissions were a strong function of engine speed. The particle number emissions are likely a stronger function of particle number emissions on the freeway due to the release of particles from the walls of the engine cylinders and exhaust system which occurred at high engine speeds and exhaust flows (Mathis et al., 2005).

3. In all three road types, exhaust temperature had a negative effect on number emissions, although it was not significant in the rural section. Low exhaust temperatures can encourage the formation of nucleation mode particles from gaseous hydrocarbons from DOC-equipped diesel buses (Rönkkö et al., 2006). The effect of exhaust temperature on mass emission rates is mixed, with high exhaust temperatures both favoring and discouraging particle mass emission rates.

4. Fuel rate is a more reliable predictor of both particle metrics than engine speed. The Fuel, $Fuel^2$ and $Fuel_{t-1}$ coefficients have more consistent values across facility types than engine speed and exhaust temperature. The other coefficients add significant predictor information, but are much more affected by different driving conditions on each facility type. Particles formed from hydrocarbons in the fuel and lubricating oil, are better linearly related to the fuel rate. Additionally, engine speed can remain high during deceleration events and does not linearly converge to zero at low loads. Using fuel-based emission factors (Zhang et al., 2005), which assume linear relationships between particles and fuel, (i.e. particles/kg fuel) is a reasonable method to estimate particle emissions, although the ratios will likely change between road types and operating modes.

Conclusions

For the bus studied, the particle number and mass emissions are positively correlated throughout a route, both temporally and spatially. However, statistical models confirmed several differences of behavior for particle number and mass emissions during real-world bus operation. Particle mass emissions were more sensitive to high fueling events that occurred at high grade segments and accelerations on the freeway. Particle number emissions were more influenced by high engine speed and short accelerating events, likely due to the storage and release of ultrafine particles. Both metrics were most consistently correlated to fuel rate.

To limit particle exposure, transit authorities could implement several practices. 1. By eliminating unnecessary accelerations (through priority intersections or exclusive bus lanes), DOC-equipped buses could significantly reduce particle exposure in terms of number and mass. 2. While acceleration events dominate emissions for typical bus stops, idling can be significant if the bus idles for several minutes. Enforcement of anti-idling policies can have a significant benefit on both particle number and mass emissions. 3. The cleanest buses should be used on the routes that have the highest population exposure and the highest distance-based emission rates. For the evaluated bus routes the selection would not be straightforward, as the freeway route had the highest average distance-based particle emission rate, but the intersections on the urban and rural arterial had the maximum distance-based emission rates. We would recommend using the cleanest buses on the urban arterials, because of the close proximity of pedestrians and urban residents to the roadway. The divided freeway has a larger shoulder, allowing more time and distance for high particle number concentrations to decay before reaching populated areas offset from the freeway.

Comparison of results to previous studies

The particle emission rates and particle size distributions were compared to other particle emission studies to verify their validity. In this work, the mean values for the dominant road types ranged from 1.2E+14 particles/km on the rural arterial to 2.7E+14 particles/km on the divided highway. These values are somewhat lower than the mean particles/km emission rate of 3.08E+14 reported in the review by Morawska et al. (2008) for diesel transit buses.

The particle mass emission rates in our study ranged between 19 mg/km on the rural arterial and 38 mg/km on the freeway, which are almost an order of magnitude lower than should be expected. Lanni (2003) reported mass emission rates for New York City transit buses tested on chassis dynameters between of 90 and 400 mg/km for conventional buses with diesel oxidation catalysts, and between 5 and 25 mg/km for buses equipped with diesel particle filters (DPF). Thus, our measurements appear to be unrealistically low, and compare better with DPF-equipped buses. Comparison in absolute particle number and mass with other studies should always be seen as approximate due to different particle measurement instruments, dilution techniques, diesel buses, testing conditions, fuel types, and driving cycles/operating conditions. However, the Lanni (2003) measurements are typical of conventional diesel vehicles (Prucz et al., 2001, Robert et al., 2007) and diesel particle filter-equipped vehicles (Biswas et al., 2008).

The particle concentration measurements from the ELPI, SMPS and gravimetric filter are consistent with one another, and are deemed valid for comparing the relative variability of particle number and mass measurements. The unrealistically low emission rates could be due to measurement errors of the dilution ratio. Underestimating the dilution ratio would have caused the emission rates to be systematically lower, even if the particle concentrations measurements were correct (Equation 1). Other studies have reported difficulty in calculating accurate dilution ratios in both artificial dilution tunnels (Clark et al., 2007) and chase-plume studies (Kittelson et al., 2006a).

The particle size distributions measured in this work compare well with previous heavy-duty diesel emission studies that measure particles in artificial dilution tunnels. The particle number size distribution has both a variable nucleation mode, and a repeatable accumulation mode, with the peak of the accumulation mode occurring between 60 and 100 nm (Shi et al., 2000, Vaaraslahti et al., 2004, Liu et al., 2007, Ristovski et al., 2006). The particle mass distributions have a single peak in accumulation mode occurring between 100 and 180 nm (Robert et al., 2007).

The particle size distributions in our study frequently showed the presence of a nucleation mode. However, the artificial dilution conditions and sampling system may have underestimated the nucleation mode concentration. Recent vehicle chase studies of heavy-duty diesel exhaust revealed that a large nucleation mode is often present in the exhaust plume, below 10 or 20 nanometers. The nucleation mode concentration dominates the total number of particles, with a peak concentration of 1 to 2 orders of magnitude higher than the peak accumulation mode concentration (Kittelson et al., 2006a, Rönkkö et al., 2006). Figure 5.2-6, gives evidence that the nucleation mode is larger than is measured by the ELPI. The SMPS coincided with the ELPI measurements, and also may have missed a significant nucleation mode peak, because the SMPS only measured particles down to 10 nm (Vikara and Holmen, 2006). Rönkkö et al. (2006) concluded that instruments that only measure down to 10 nm would miss or seriously underestimate nucleation mode particles.

The nucleation mode may have been suppressed in our measurements by the mini-dilution system, because dilution conditions that favor large nucleation mode formation are difficult to replicate using an artificial dilution tunnels (Kittelson et al., 2006a, Rönkkö et al., 2006). Two emission processes were shown to contribute to the formation of a large nucleation

mode from a DOC-equipped diesel transit bus (Rönkkö et al., 2006). At low engine loads and exhaust temperatures, the nucleation mode is comprised of unburned hydrocarbons from the fuel and lubricating oil. At high loads, the nucleation mode is comprised of sulfates that were oxidized at high exhaust temperatures in the diesel oxidation catalyst. The consistent negative effect of exhaust temperature on particle number emissions in our results (Table 5.2), suggests that a sulfate-based nucleation mode was suppressed or undetected by the measurement equipment. The mini-dilution used in our study was previously shown to suppress nucleation mode formation for particles from a DPF-equipped and CNG vehicles (Holmen and Ayala, 2002).

Small particle losses may have contributed to an underestimation of the nucleation mode particles in the mini-dilution sampling system. Particle losses due to diffusion in the sampling line system and measurement equipment can dominate small particle measurements. Kittelson et al. (2006a) found that the measured particle number concentration were four times smaller than the actual concentration in the exhaust, due to small particle losses. The ELPI corrects for small particle losses, but no corrections were made for particle losses within the sampling lines and mini-dilution system (Holmen et al., 2005).

The formation of nucleation mode is complex, and the understanding of the underlying mechanisms of formations is rapidly changing. Even though the nucleation mode may have been suppressed from our data, the measurement methods and results are consistent with the current state of practice. For example, Ristovski et al. (2006) measured diesel transit bus emissions using a chassis dynamometer and artificial dilution tunnel, but rarely detected a significant nucleation mode when operating on ultralow sulfur diesel fuel. Additionally, no protocol has been established for measuring nucleation mode particles and measurements can be substantially different based on sampling conditions and the sampling equipment. The European Union has established a particle measurement procedure (PMP) used to establish a particle number based standard. The PMP removes the volatile fraction of the exhaust, which is responsible for the formation of the nucleation mode, in order to maintain repeatable results (Morawska et al., 2008). Ideally, sampling methods should repeatedly measure the true magnitude of nucleation mode particles that exist in the exhaust plume from vehicles driving in real-world measurements, however such measurement methods are still evolving for artificial dilution systems (Rönkkö et al., 2006, Kittelson et al., 2006a).

In summary, the particle size distribution measurements made in this study are consistent with the state of practice. However, the data should be used with the qualification that a large nucleation mode for particles smaller than 30 nm may have been suppressed by the artificial dilution and sampling system. The particle mass distributions are less sensitive to dilution conditions, and are consistent with other studies. The absolute concentration of particle number and mass concentration were lower than should be expected for a conventional diesel bus, which likely reflects an error in the dilution ratio measurements. The relative variation of particle number and mass instruments are valid for the qualifications given, however the absolute concentration of the particle number and mass emissions are likely invalid and should not be used to compare with other studies.

This is the first known study measuring particle number emissions with an on-board dilution system. Future work is needed to assure that particle number measurements made in artificial dilution tunnels compare well with real-world exhaust plumes. Additional research is needed to better quantify the contribution of particle number and mass emissions from a larger set of vehicles, including low-emission diesel vehicles in transient operating conditions. Even though the data from this study may have limited application, the presented analysis provides a useful framework for analysis of complex real-world emissions. In depth exploratory analysis,

coupled with statistical analysis across two days of testing was a useful strategy to extract useful conclusions about the variation of particle number and mass emission rates.

Acknowledgments

We gratefully acknowledge Zhong Chen and Derek M. Vikara for conducting the field measurements, Eric D. Jackson for assistance with data processing and providing insights for analyzing the data, and Yiannis Kamarianakis for giving statistical methods advice. This research was sponsored by the New York Metropolitan Transportation Council and University Transportation Research Council through the September 11th Program Fellowship Program, the New York State Energy Research Development Authority through the Environmental Monitoring, Evaluation, and Protection PhD Fellowship Program, the Joint Highway Research Advisory Council of the University of Connecticut, and the Connecticut Department of Transportation through Projects 03-8 and 05-9.

APPENDIX

Table 5.A1. Summary Statistics of Each Road Type (September 20th)

Roadway type	Time, m:s	Distance, km	Mean speed , km/ hr (min/max)	Stops	Mean grade, % (min/max)
Divided Highway	15:32	24.5	95 (18/110)	0	-0.04 (-3.3/4.1)
Rural Arterial	12:16	10.1	19 (0/61)	3	-0.5 (-8.5/9.0)
Urban Arterial	39:22	12.7	49 (0/84)	38	-0.5 (-6.7/5.6)
Overall	67:10	47	42 (0/110)	41	-0.3 (-8.5/9.0)

Table 5.A2. Time-Based Emission Rates for September 20th

Road Type	Number (#/sec)		Mass (mg/sec)		Correlation R^2
	Mean	CV	Mean	CV	
Divided Freeway	7.0E+12	0.44	1.00	0.55	0.54
Rural Arterial	1.7E+12	1.11	0.26	1.7	0.62
Urban Arterial	9.2E+11	1.36	0.11	1.6	0.81
Overall	2.48E+12	1.29	0.34	1.49	0.80

Table 5.A3. Time-Based Emission Rates for September 21st

Road Type	Number (#/sec)		Mass (mg/sec)		Correlation R^2
	Mean	CV	Mean	CV	
Divided Freeway	6.63E+12	0.51	1.34	0.63	0.70
Rural Arterial	1.30E+12	1.17	0.24	1.75	0.71
Urban Arterial	6.92E+11	1.57	0.10	1.88	0.83
Overall	2.12E+12	1.45	0.40	1.70	0.86

Table 5.A4. Distanced-Based Emission Rates for each 50 meter Segment on September 20th

Road Type	Number (#/km)		Mass (mg/km)		Correlation R^2
	Mean	CV	Mean	CV	
Divided Freeway	2.6E+14	0.38	37.5	0.51	0.49
Rural Arterial	1.2E+14	1.20	18.5	1.8	0.65
Urban Arterial	1.7E+14	1.03	18.9	1.5	0.87
Overall	2.0E+14	0.86	28.0	0.82	0.70

Table 5.A5. Percentiles for Distance-based Particle Emission Rates for Sep. 20th

	Number/km			**Micrograms/km**		
Percentiles	**50m**	**100m**	**200m**	**50m**	**100m**	**200m**
5	4.7E+11	8.9E+11	8.9E+11	0.1	0.1	0.6
10	1.1E+13	2.2E+13	2.2E+13	1.0	1.5	3.0
25	8.1E+13	9.9E+13	9.9E+13	6.1	8.3	8.7
50	2.1E+14	2.2E+14	2.2E+14	19.4	22.2	24.3
75	2.9E+14	3.0E+14	3.0E+14	44.5	45.2	42.4
90	3.9E+14	3.9E+14	3.9E+14	61.4	60.7	57.5
95	4.3E+14	4.2E+14	4.2E+14	76.4	71.6	67.7
99	6.8E+14	5.5E+14	5.5E+14	107.6	105.7	102.7

Table 5.A6. Summary Statistics on all (42) of the 50-meter Episodes that included stops.

	Deceleration	Idle	Acceleration
Mean time, s	7.46	16.1	7.3
Median time ,s	7	9	8
Minimum time,s	2	1	0
Maximum time, s	15	81	13
Total time in all 50 meter segments, m:s	5:05	11:00	5:21
Mean particle number emission rate, #/s	1.4E+11	1.6E+11	2.1E+12
Sum, total number, #	4.4E+13	1.0E+14	6.8E+14
Percent contribution of particle number emissions	5.3%	12.7%	82.0%
Mean particle mass emission rate, ug/s	27.8	50.0	275.4
Sum, mass emissions, mg	8.49	33.0	88.4
Percent contribution of particle mass emissions	6.5%	25.4%	68.1%

Table 5.A7. Model Coefficients for September 21st

	1. Urban Model		**2. Rural Hill Model**		**3. Freeway Model**	
Parameter	Number	Mass	Number	Mass	Number	Mass
Intercept	-0.33	-0.43	-0.26	-0.52	-0.55	-0.84
Fuel	0.16	0.12	0.36	0.09	0.26	-0.08
$Fuel^2$	0.10	0.22	-0.08	0.09		0.28
$Fuel_{t-1}$	0.28	0.19	0.21	0.11	0.36	0.54
Engine Speed	0.30	0.15		-0.12	0.52	-0.09
Engine $Speed^2$	0.17	0.07		1.04	0.73	0.44
Engine $Speed_{t-1}$	-0.04	-0.07				
Exhaust Temperature	-0.04			-0.02	-0.70	0.18
Fit Statistics						
Adjusted R^2	0.96	0.93	0.95	0.99	0.85	0.84

Table 5.A8. Operation Mode Definitions for Table 5.1

Road type	Operating Mode	Acceleration, kmh/s	Vehicle Speed, kmh	Grade, %
Urban Arterial	Acceleration	>= 0	< 40	
	Acceleration	>= 1	>= 40	
	Deceleration	< 0	< 40	
	Deceleration	<-1	>= 40	
	Cruise	(-1,1)	>= 40	
	Idle		= 0	
Rural Arterial	Acceleration	>= 0	< 40	
	Deceleration	< 0	< 40	
	Uphill cruise		>= 40	>= 1
	Downhill cruise		>= 40	=< -1
	Level cruise			(-1,1)
	Idle		= 0	
Divided Freeway	Acceleration	>= 1	< 40	
	Deceleration	=< -1	< 40	
	Cruise	(-1,1)		

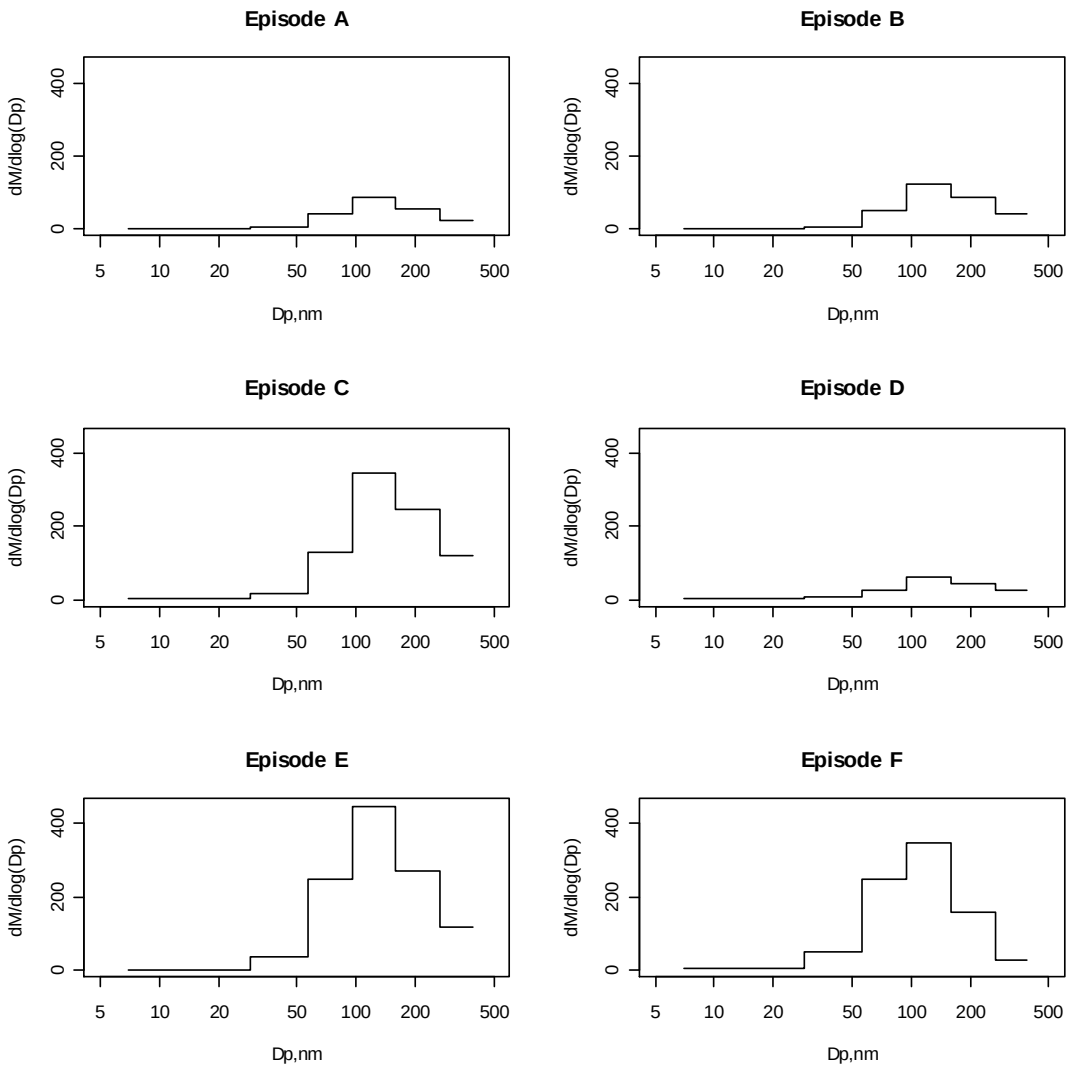

Figure 5.A1. Mean mass-distributions for selected episodes. Units for mass concentrations are in ug nm^{-1} m^{-3}. Only particles in the lower 6 stages (diameter < 387 nm) are used to compute mass concentrations.

ELPI-derived number emissions rate

To compute temporally resolved particle number emission rates, the particle concentration data and the exhaust flow rate was synchronized to the engine data. This was required because of the different clock-times on the instruments and to account for the time needed for the aerosol to travel from the engine through the exhaust and dilution systems to the ELPI. To align the data, the lag between the engine and ELPI was estimated by observing the initial engine start and initial spike in particle concentration. Then the lag that produced a maximum cross-correlation between the engine speed (RPM) and particle concentrations was calculated. The temporal shift that produced the best correlation between engine speed and particle concentrations and was consistent with the observed lag was used to synchronize the particle concentration measurements to the engine data. Similarly, a temporal shift was applied to synchronize the exhaust flow rate to the engine data. Once all the data were temporally aligned to the engine data, the particle number emissions rate was calculated using equation 1.

ELPI-derived mass emissions rate

One of the key disadvantages of the filter measurements is aggregate time resolution. In this study, mass-weighted particle size distributions and concentrations were derived from ELPI particle measurements, as has been done in other studies (Kinsey et al. 2006; Maricq et al., 2006;; Shi et al., 2000). To illustrate the calculations, the particle mass distribution was calculated for a one minute period on the urban arterial section. The ELPI measured 31 observations during this one minute period. During the minute period, the bus was traveling between 20 and 37 mph, with engine load ranging between 0 and 100%. The number-weighted, average particle size distribution in terms of dN/dlogDp for the 31 observations is plotted in Figure 5.A2a., showing that the majority of particles are below 100 nm.

Initially, the mass-weighted size-distribution was calculated by using all 12 ELPI stages, using a straightforward approach assuming that all the particles were unit density spheres with diameters equal to the geometric mean of each stage. The particle mass density was computed in terms of dM/dlog(Dp) in Figure 5.2b. The average mass distribution is dominated by particles in the upper two stages (particles > 2.42 um) suggesting that the mass is dominated by coarse mode particles. However, the mass-weighted particle size distribution for diesel exhaust is typically dominated by the accumulation mode around 100 nm (Kittelson, 1998; Burtscher, 2005). In Figure 5.2c the observations that had readings in the upper two stages were removed, showing that most observations have a characteristic accumulation mode around 100 nm. For the entire data set, only 30% of the ELPI measurements recorded readings in the stages 11 and 12, yet these readings contribute to over 75% of the total mass.

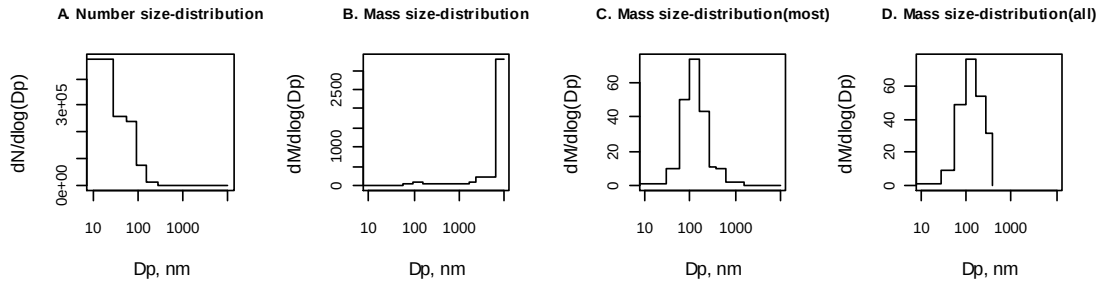

Figure 5.A2. Average particle size distributions for a one-minute period (31 observations) along the urban arterial. A. Number-weighted particle size distribution averaged for all 31 observations. B. Mass-weighted particle size distribution averaged for all 31 observations. C. Mass-weighted particle size-distribution for the 20 observations with no coarse mode particles. D. Mass-weighted particle size-distribution for all the observations, but excluding the all particles above 387 nm.

The large mass in the coarse mode is believed to be an erroneous measurement from the ELPI. Other researchers have observed similar phenomenon, concluding that summing over all 12 stages of the ELPI can lead to significant over estimation of the PM mass concentrations of diesel exhaust (Kinsey et al., 2006; Maricq et al., 2006; Shi et al., 2000). The overestimation occurs due to positive artifacts that occur on the upper stages of the ELPI (Maricq et al., 2006). More accurate mass concentrations have been obtained by only using the bottom 5 stages (Kinsey et al., 2006). Maricq et al. (2006) has proposed an iterative algorithm that uses the measurements from all 12 stages and assumed properties for diesel agglomerates (i.e. lognormal distribution, mobility densities) to estimate a particle mass distribution from ELPI data. The algorithm has yielded errors within 20% compared to gravimetric filter based measurements.

In this study we used the lower stage approximation for simplicity in calculating mass concentrations for a large amount of data. In Figure 5.2d, the mass distribution is plotted by only including the bottom 5 stages and the electrical filter stage. By so doing, the data has a characteristic accumulation mode similar to the observations without inflated coarse-mode readings.

The accuracy of computing the total mass concentration from using the lower stages of the ELPI was evaluated by comparing it to the filter measurements. The average mass concentration was computed by assuming the particles were unit density spheres, with diameter equal to the geometric mean of each stage, yielding the following summation across the 6 stages:

$$M\left(\frac{\mu g}{m^3}\right) = \sum_{i=1}^{6}\left(\frac{\pi}{6}\right)\cdot\rho_o\cdot\overline{D}_i^3\cdot\Delta N_i\cdot DR_A$$

The average mass concentration over each route was compared to the average mass concentration derived from the gravimetric filter measurements. For the routes measured on September 20th and 21st, the ELPI and filter mass measurements correlated by an R^2 of 96% and the ELPI were 15% larger than the filter measurements (Figure 5.A3). Given that gravimetric mass filter measurements are also prone to error (e.g. hydrocarbon absorption on the filter, (Maricq et al., 2006). The strong correlation between the two measurements gives credence to the ELPI-derived mass concentrations.

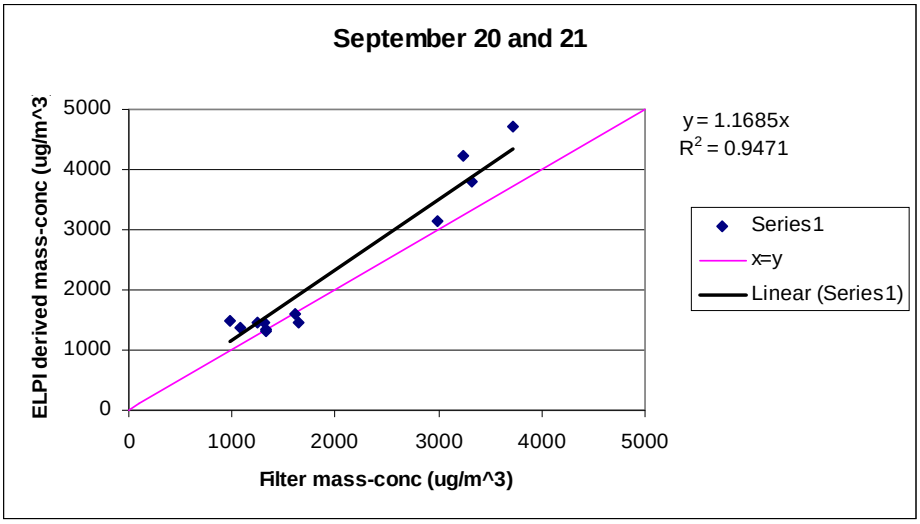

Figure 5.A3. Comparison of particle mass concentrations derived from the ELPI and gravimetric filter. The mass concentrations are the route-averages for 16 routes measured on September 20th and September 21st.

Comparisons of the two approaches for all the available conventional diesel bus tests from the Holmén et al. (2005) study are plotted in Figure 5.A4, which includes results from 62 test runs over 8 days on two conventional diesel buses. The ELPI–derived PM mass emissions are correlated with the filter-based PM mass concentrations with a R^2 coefficient of 76%. On average the ELPI derived-mass measurements are 16% larger than the filter mass concentrations. The higher PM mass results from ELPI-based calculation could be due to the unit density assumption which tends to be too high based on ELPI measurement (Shi et al., 2000).

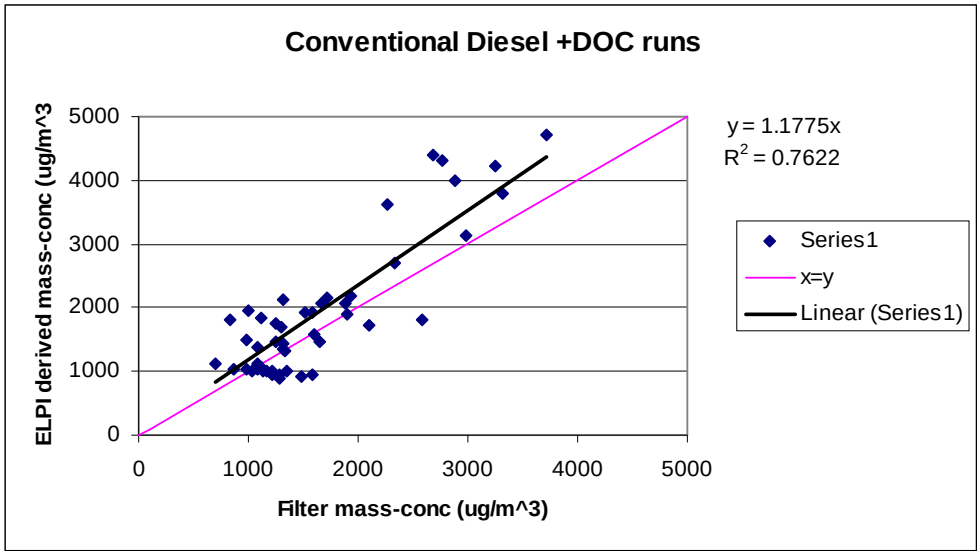

Figure 5.A4. Comparison of ELPI derived mass concentrations and gravimetric filter mass concentrations for the 62 bus routes tested with conventional diesels.

Particle number and mass measurements with the bus equipped with a diesel particle filter

As part of the Holmén et al. study (2005) the diesel bus was equipped with an Engelhard DPX diesel particle filter for the last phase of testing. The bus was tested on the same test run in Hartford CT for two days: November 9th and 10th of 2004. The route-average particle number concentrations were reduced by over 99% by the diesel particle filter. Previous studies evaluating the effectiveness of diesel particulate filters on diesel transit buses have shown similar reductions in the particle number concentration by one to two orders of magnitude (90~99%) (Holmén and Ayala, 2002 ; Lanni, 2003; Holmén and Qu, 2004; Nylund et al., 2004. The SMPS also recorded substantial reductions (between 95 to 99%) in particle number emissions with the use of the diesel particulate filter (Vikara and Holmén, 2006).

However, recent research has shown that diesel particle filters equipped with catalysts (DOCs) can increase the number of ultrafine particles, because the catalyst and removal of accumulation mode particles by the filter favors the nucleation of sulfates (Biswas et al. 2009). This phenomenon has been observed from testing an Engelhard DPX filter (Biswas et al. 2008). As discussed previously, the nucleation mode may have been suppressed by the mini-dilution system (Holmén and Ayala, 2002) and the nucleation mode particles may have been smaller than the detectable range of the ELPI (Rönkkö et al. 2006).

An in-depth comparison of the particle number and mass measurements was desired for the DPF-equipped bus. The same methodology was applied to derive the mass concentrations from the lower stages of the ELPI measurements, and the results are plotted in Figure S5.A5. The ELPI measured reductions in the particle mass concentration of more than 99%, while the filter measurements reported the post-DPF mass concentrations were reduced by only 73%.

The particle mass concentrations derived from both instruments are plotted on Figure 5.A5. During these tests, the ELPI-based mass concentrations were less than 3% of the filter-based concentrations and had an R^2 correlation coefficient close to zero (Figure 5.A5). The inconsistency between the mass concentrations for the post-DPF runs may have occurred due to hydrocarbon adsorption on the gravimetric Teflon filter (Maricq 2006), and because the concentrations of particles were near the detection limit of both the ELPI and the Teflon filter (Holmén et al. 2005). Additionally, the ELPI and SMPS may have not detected sulfate particles that could have contributed to a significant portion of the mass for the DPF-equipped bus.

Because the accuracy of neither the ELPI nor filter-based measurements can be assured from the post-DPF test runs, the post-DPF runs were not further analyzed.

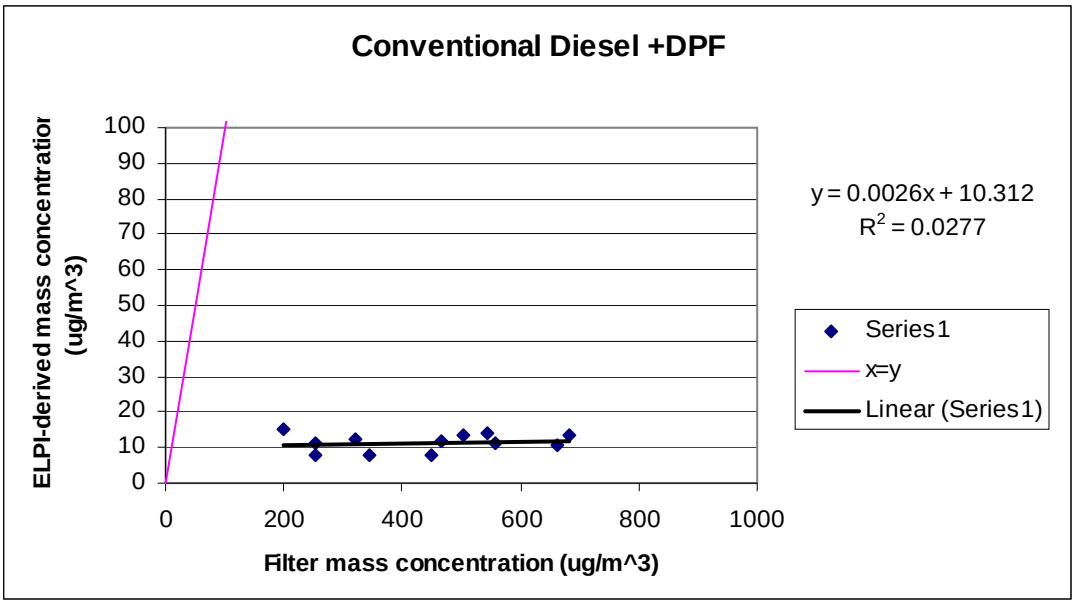

Figure 5.A5. Comparison of ELPI derived mass concentrations and gravimetric filter mass concentrations on November 9th and 10th when the bus was equipped with a DPF.

Negative and Low Exhaust Flow Rates

The emission rates depend on the accurate measurements of emissions concentrations and total exhaust flow rate. The exhaust flow rate was measured from a pitot tube assembly included in the Horiba gas analyzer. Obtaining reasonable exhaust flow rates was problematic, and during the first months of testing large amounts of negative exhaust flow rates were recorded. In an effort to solve the problem of low exhaust flow rates, an extension on the tail-pipe was built to prevent wind-backflow, and the pitot tube was re-zeroed after each testing route (Holmén et al. 2005). Even still, the Horiba frequently recorded unreasonably low and negative exhaust flow readings. For the 8 days of testing runs of the conventional diesel buses, more than 1 in 20 observations on the urban arterial had a negative exhaust flow rate recorded. Most of these observations (over 65%) occurred when the bus was idling.

To correct for the negative and unreasonably low exhaust flow values, a minimum exhaust value of 1300 L/min was set. 1300L/min was chosen because it was the median value for exhaust flow rate for the bus during idle during bus routes that did not have significant amounts of negative exhaust flow rates. Theoretically, the minimum exhaust flow rate at idle can be calculated from the engine speed, which is roughly 700 rpm for the analyzed transit bus. The diesel engine intakes and vents the cylinders once every two cycles, yielding the following equation:

$$Exhaust\ \ flow = Engine\ displacement \times Engine\ speed \times volumetric\ efficiency \times \left(\frac{1}{2}\right)$$

$$2100\ L/\mathrm{m} = 8.7L \times 700\ rpm \times 0.7 \times \left(\frac{1}{2}\right)$$

This minimum exhaust flow rate should be seen as an approximate, "back of the envelope" estimate. The volumetric efficiency is assumed to be 0.7, no consideration is given to

the fuel rate, which should be a minor contribution of exhaust flow at low fuel rate, and the exhaust gas is assumed to be at constant pressure and temperature between the cylinder and exhaust flow measurements. However, this is not the case due the turbocharged engine. Regardless, it appears that we are warranted in setting a minimum exhaust flow rate to correct for the low and negative exhaust flow rates. The 1300 L/min is smaller than 2100 L/min but will be retained for two reasons. Because it is derived from the Horiba values it is more consistent with the other exhaust flow measurements. Additionally, we do not have any data on the true volumetric efficiency constant for the bus at idle, and the exhaust flow calculation is only approximate.

For the September 20th runs evaluated in detail in the report, 10.7% of the exhaust flow values are under the minimum value of 1300 L/min. Of these 64.5% of these occur in the idling mode, which consists of 42% of all the idling values. Another 22% of the low exhaust values occurred during low speed decelerations, while another 12% occurred during low speed cruising modes. Because there is anticipated to be considerable variability in the exhaust flow rates within these operating modes, using a larger value than 1300 L/min value, would eliminate a larger portion of the emission rate variability.

The sensitivity of the results was examined by setting the somewhat arbitrary minimum exhaust flow rate of 1300 L/min. The overall mean of the September 20 emission rates for particle number and mass only increased slightly. For the divided highway section, there was no change due to the high exhaust flow rates. On the urban arterial the number emission rates increased by 1.2% and the mass emission rates increased by 3.2%. The other routes had changes less than 1%. The overall share of idling emissions increased from 0.9% to 1.1% for number emissions and from 1.9% to 2.4% for mass emissions. The emission rates were not highly sensitive to the emission rate changes. Overall, we are interested in the high emission events which have exhaust flow rates far above 1300 L/min, so our results and conclusions will not be very sensitive to the selected minimum exhaust flow rate.

Cold Start

All data analyzed in the report were measured with the warmed up transit bus. To examine if cold-start idling had high emission rates, the cold-start recorded from September 21 was analyzed. The mass emission rate was 0.029 mg/sec and number emission rate was 1.29e+11 particles /sec. The mass emission rate was 42% smaller than the mean idle emission rate for the entire route on September 20th, and the number emission rate was 26% smaller than the mean idle emission rate. Mathis et al. (2005) examined cold start emissions from diesel and spark ignition vehicles. For the diesel engine (with oxidation catalyst) the cold start had almost no effect on the idling emission rates in terms of particle emissions. Even though only one cold start was analyzed, our data confirm previous results, that cold-start idling does not have a significant impact on particle number of mass emission rates for a conventional diesel bus.

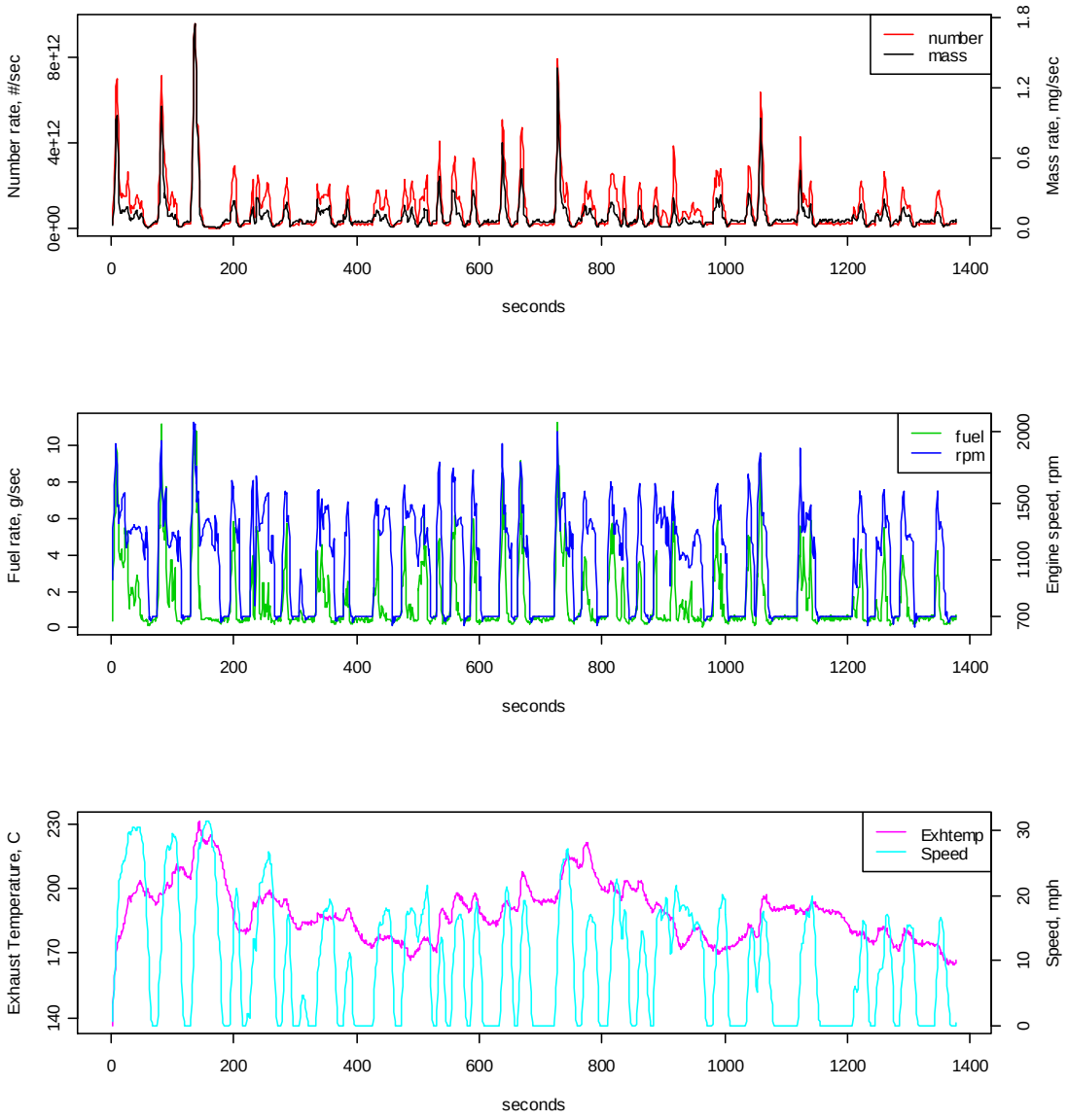

Figure 5.A6. Particle emissions and covariates for modeled urban arterial section.

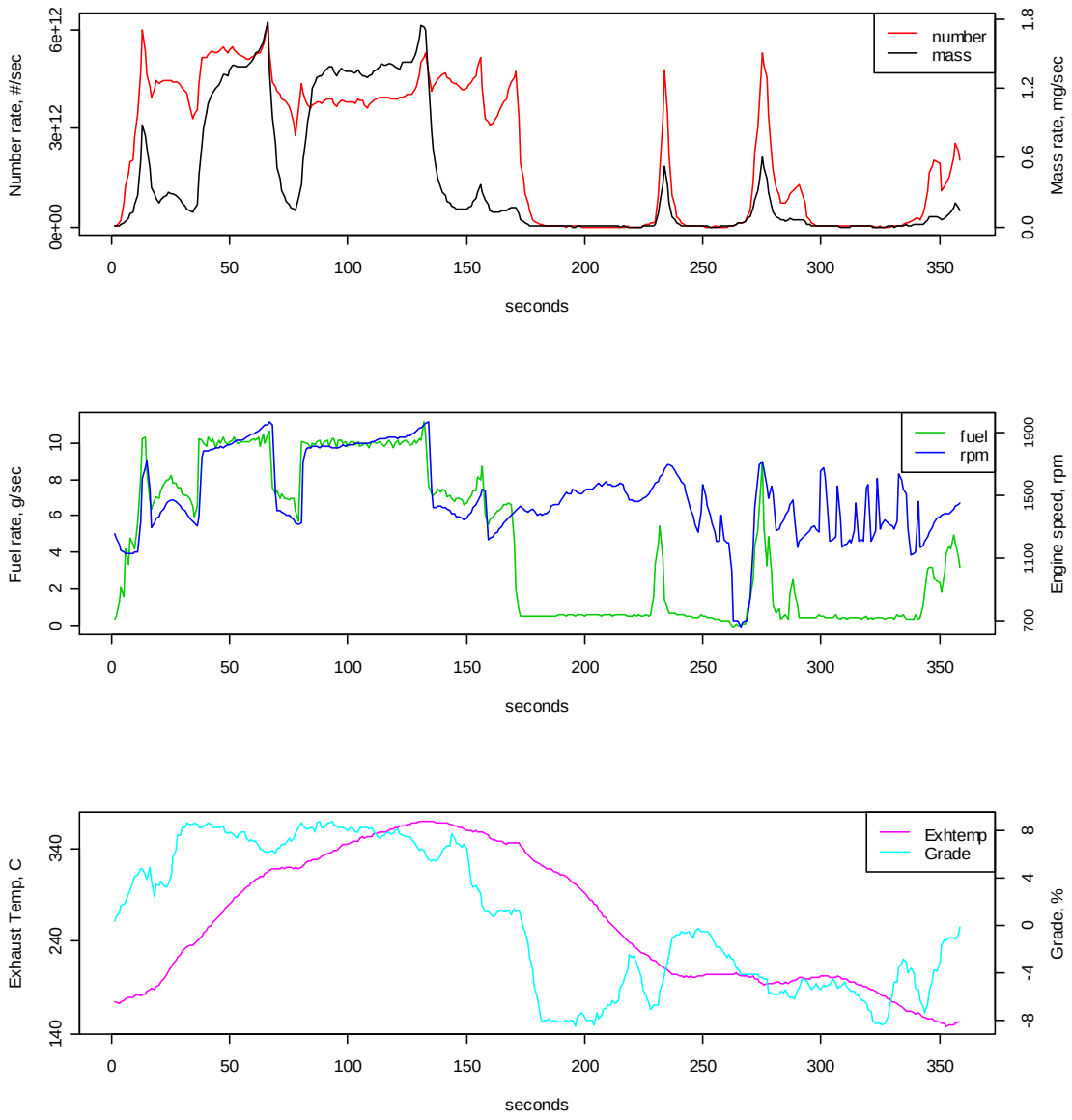

Figure 5.A7. Particle Emissions and covariates for modeled rural arterial section.

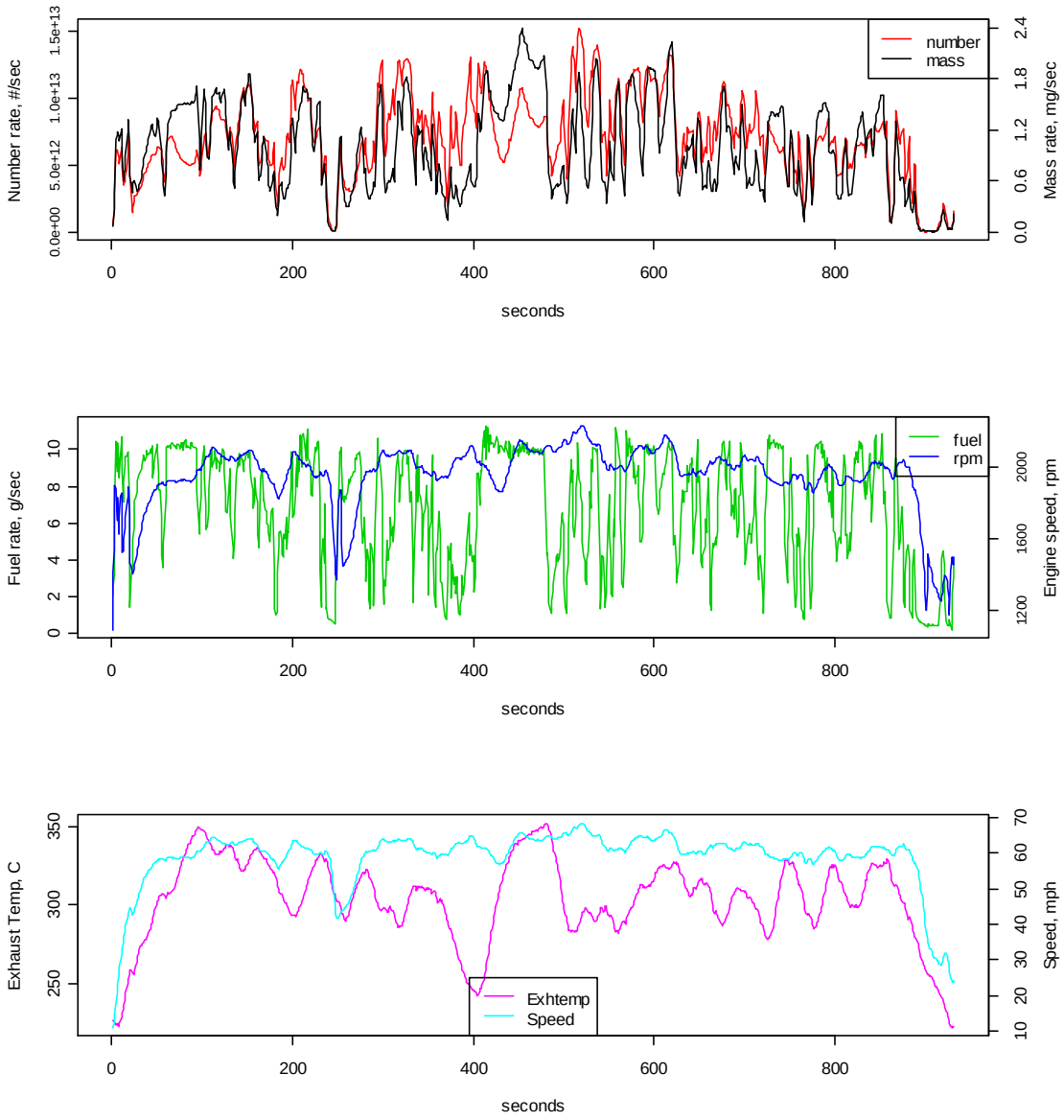

Figure 5.A8. Particle Emissions and covariates for modeled divided freeway Section.

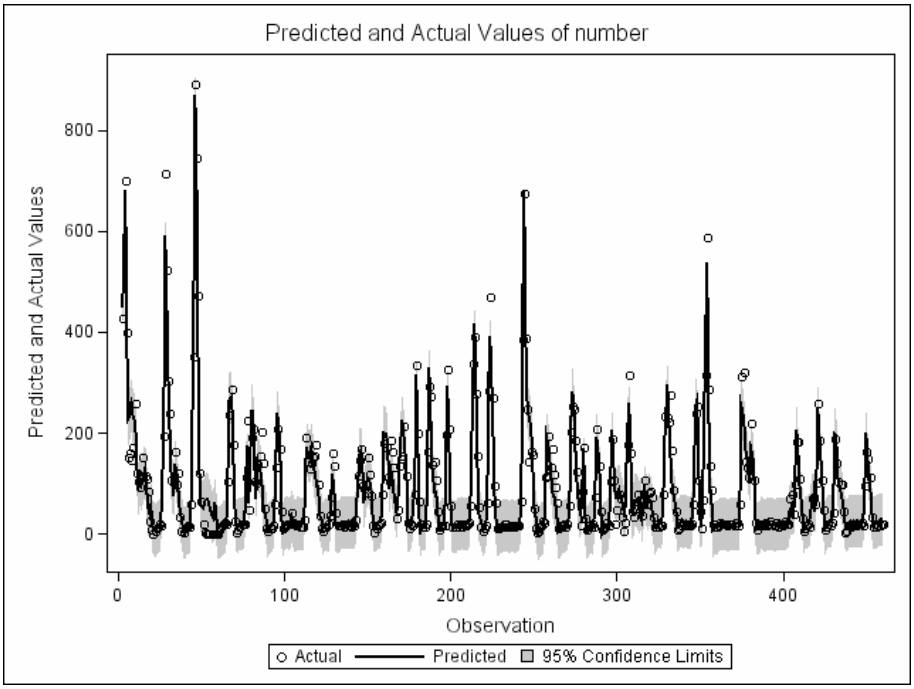

Figure 5.A9. Predicted and actual values for particle number emissions on urban arterial section.

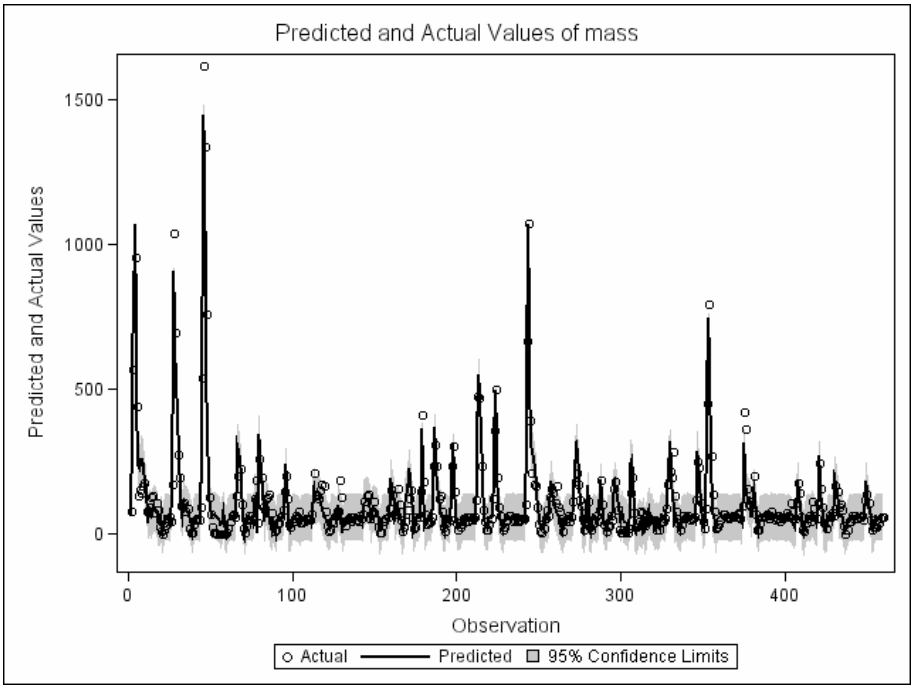

Figure 5.A10. Predicted and actual values for particle mass emissions on urban arterial section.

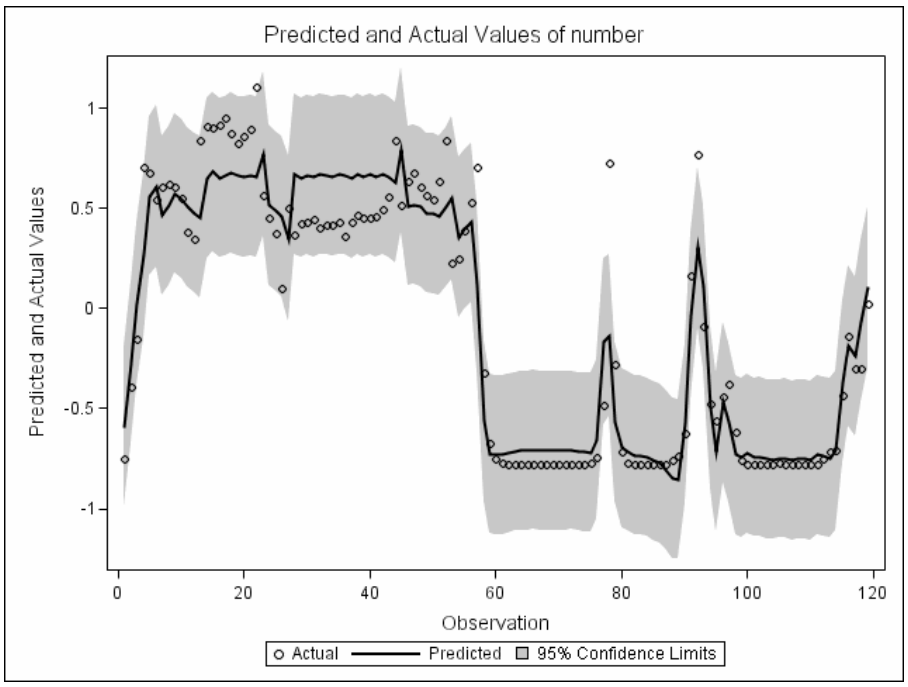

Figure 5.A11. Predicted and actual values for particle number emissions on rural arterial section.

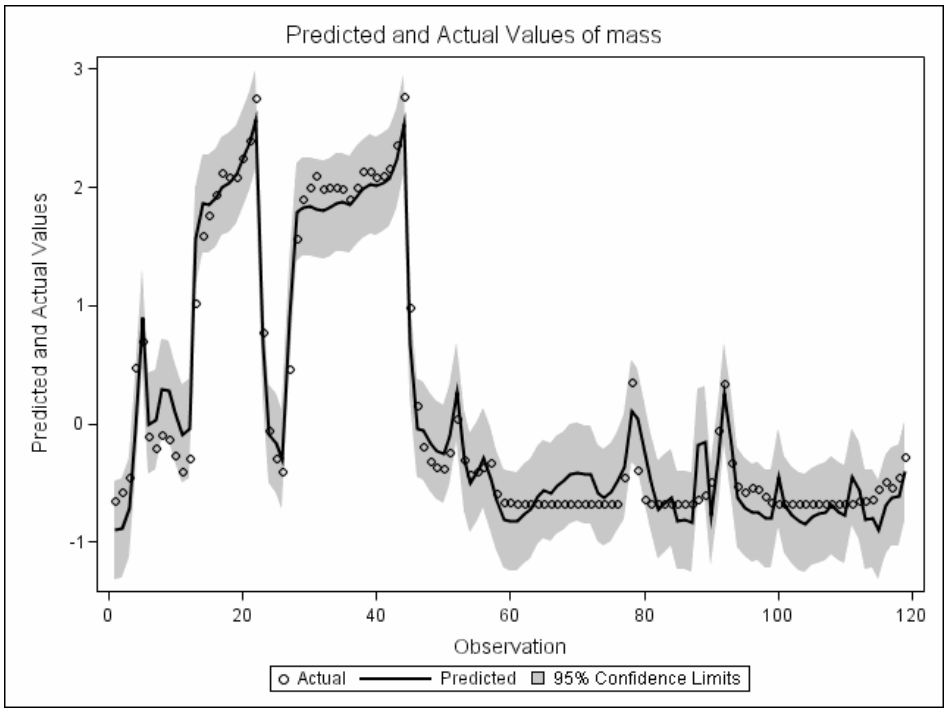

Figure 5.A12. Predicted and actual values for particle mass emissions on rural arterial section.

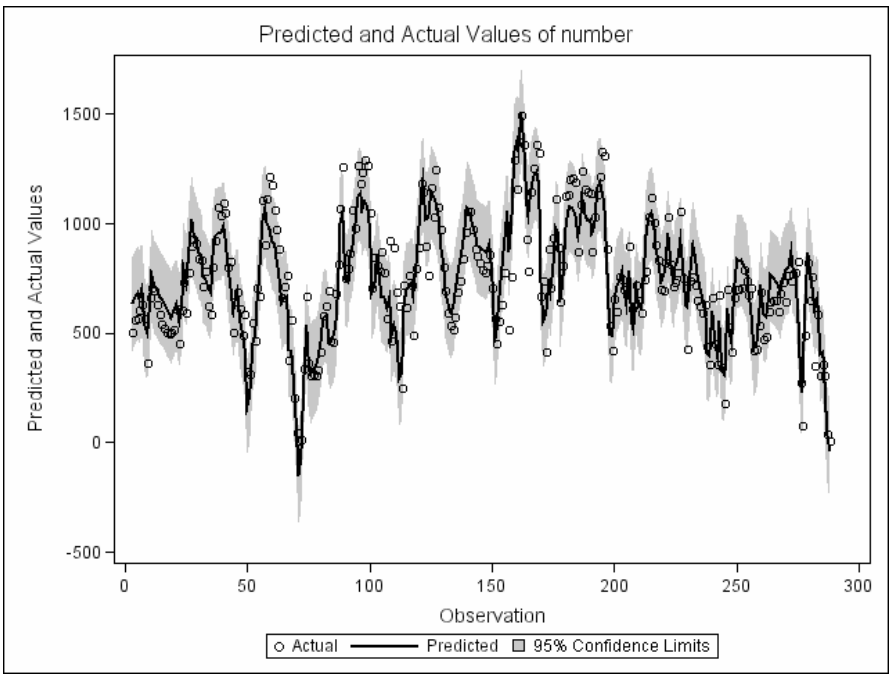

Figure 5.A13. Predicted and actual values for particle number emissions on divided freeway section.

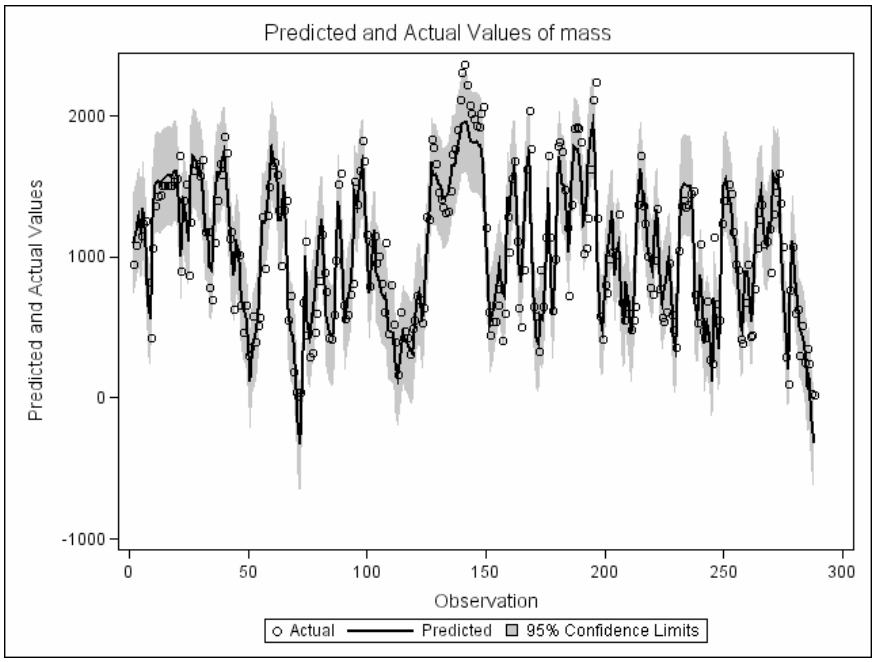

Figure 5.A14. Predicted and actual values for particle mass emissions on divided freeway section.

REFERENCES

American Lung Association (ALA): State of the Air 2007. Available at http://www.lungusa.org.

Baltensperger, U.; Weingartner, E.; Burtscher, H. Dynamic Mass and Surface Area Measurements. In *Aerosol Measurement - Principles, Techniques, and Applications (2nd Edition)*. Baron, P. A.; Willeke, K. John Wiley & Sons: New York, 2001.

Baron, P. A.; Willeke, K. Bridging Science and Application in Aerosol Measurement: Accessing Available Tools. In *Aerosol Measurement - Principles, Techniques, and Applications (2nd Edition)*. Baron, P. A.; Willeke, K. John Wiley & Sons: New York, 2001.

Biswas, S.; Hu, S.; Verma, V.; Herner, J. D.; Robertson, W. H.; Ayala, A; Sioutas, C. Physical properties of particulate matter (PM) from late model heavy-duty diesel vehicles operating with advanced PM and NOx emission control technologies. *Atmospheric Environment*. **2008**, *42* (22), 5622-5634.

Biswas, S.; Verma, V.; Schauer, J. J.; Sioutas, C. Chemical speciation of PM emissions from heavy-duty diesel vehicles equipped with diesel particulate filter (DPF) and selective catalytic reduction (SCR) retrofits. Atmospheric Environment. 2009, 43 (11), 1917-1925.

Brunekreef, B.; Holgate, S. T. Air pollution and health. *Lancet*. **2002**, *360*, 233-42.

Clark, N. N.; Gautam, M.; Wayne, W. S.; Lyons, D. W.; Thompson, G., Zielinska, B. HEAVY-DUTY Vehicle Chassis Dynamometer Testing for Emissions Inventory, Air Quality Modeling, Source Apportionment and Air Toxics Emissions Inventory August 2007; CRC Report No. E55/59: Desert Research Institute (Subcontractor),: West Virginia University Research Corporation, Department of Mechanical & Aerospace Engineering: Morgantown, WV, 2007.

Clean Air Task Force (CATF), 2005. Diesel and Health in America: The Lingering Threat.

Harrison, R. M.; Shi, J. P.; Xi, S.; Khan, A.; Mark, D.; Kinnersley, R.; Yin, J. Measurement of number mass and size distribution of particles in the atmosphere. In *Ultrafine Particles in the Atmosphere*; Brown, L. M., Collings, N., Harrison, R. M., Maynard, A.D., Maynard, R.L., Eds.; Imperial College Press: London, 2000.

Hofeldt, D. L.; Chen, G. *Transient particulate emissions from diesel buses during the central business district cycle*. SAE Technical Paper Series 960251; SAE International. International Congress and Exposition: Detroit, Michigan, 1996.

Holmén, B. A.; Chen, Z.; Davila, A. C.; Gao, O. H.; Vikara, D. M. *Particulate Matter Emissions from Hybrid Diesel-Electric and Conventional Diesel Transit Buses: Fuel and Aftertreatment Effects*. JHR 05-304, Project 03-8; Joint Highway Research Advisory Council: Hartford, CT, 2005.

Holmén, B. A.; Ayala, A.; Ultrafine PM emissions from natural gas, oxidation-catalyst diesel, and particle-trap diesel heavy-duty transit buses. *Environ. Sci. Technol*. **2002**, *36*, 5041-5050

Imhof, D.; Weingartner, E.; Ordóñez, C.; Gehrig, R.; Hill, M.; Buchmann, B.; Baltensperger, U. Real-world emission factors of fine and ultrafine aerosol particles for different traffic situations in Switzerland. *Environ. Sci. Technol*. **2005**, 39, 8341-8350.
Jackson, E. D., Holmen, B. A. Modal analysis of vehicle operation and particulate emissions from Connecticut Transit Buses; Transportation Research Board: Washington D.C. 2009.

Kinsey, J. S.; Mitchell W. A.; Squier W. C.; Linna, K.; King, F. G.; Logan, R.; Dong, Y.; Thompson G. J.; Clark, N. N. Evaluation of methods for the determination of diesel-generated fine particulate matter: Physical characterization results. *J. of Aerosol Science*. **2006**, *37*, 63-87.

Kittleson, D. B. Engines and nanoparticles: A review. *J. Aerosol Sci*. **1998**, *29*, 575-588.

Kittleson, D. B.; Watts, W. F.; Johnson, J. P. Nanoparticle emissions on Minnesota highways. *Atmos. Environ*. **2004**, *38*, 9-19.

Kittelson, D. B.; Watts, W.F.; Johnson, J. P. On-road and laboratory evaluation of combustion aerosols—Part1: Summary of diesel engine results. *Aerosol Science*. **2006a**, *37*, 913–930.

Kittelson, D. B.; Watts, W. F.; Johnson, J. P.; Schauer, J. J.; Lawson, D. R. On-road and laboratory evaluation of combustion aerosols—Part 2: Summary of spark ignition engine results. *Aerosol Science*. **2006b**, *37*, 931 – 949.

Lanni, T. Fine urban and precursor emissions control for diesel urban transit buses. *Environmental Pollution*. **2003**, *123*, 427-437.

Lena, T. S.; Ochieng, V.; Carter, M.; Holguin-Veras, J; Kinney, P.L. 2002. Elemental carbon and PM2.5 levels in an urban community heavily impacted by truck traffic. *Environmental Health Perspectives*. **2002**, 110(10): 1009-1015.

Liu, Z. G.; Ford, D. C.; Vasys, V. N.; Chen, D.; Johnson, T. R. Influence of engine operating conditions on diesel particulate matter emissions in relation to transient and steady-state conditions. *Environ. Sci. Technol*. **2007**, *41* (13), 4593-4599.

Maricq, M. M.; Xu, N.; Chase, R. E. Measuring particulate mass emissions with the electrical low pressure impactor. *Aerosol Science and Technology*. **2006**, *40*, 85-96.

Mathis, U.; Mohr, M.; Forss, A. Comprehensive particle characterization of modern gasoline and diesel passenger cars at low ambient temperatures. *Atmos. Environ*. **2005**, *39*, 107–117.

McCarthy, M. C.; Eisinger, D. S.; Hafner, H. R.; Chinkin, L. R.; Roberts, P. T.; Black, K. N.; Clark, N. N.; McMurry, P. H.; Winer, A. M. Particulate matter: A strategic vision for transportation-related research. *Environ. Sci. Technol*. **2006**, *40*, 5593–5599.

Morawska, L.; Ristovski, Z.; Jayaratne, E. R.; Keogh, D. U.; Ling, X. Ambient nano and ultrafine particles from motor vehicle emissions: Characteristics, ambient processing and implications on human exposure. *Atmospheric Environment*. **2008**, *42*, 8113-8138.

National Research Council. *Air Quality Management in the United States*. National Academies Press., Washington, D.C., 2004.

New York City Department of Health. Asthma Facts, Second Edition. New York City, 2003.

New York City Transit and the Environment. Metropolitan Transit Authority. Available at: http://www.mta.info/nyct/facts/ffenvironment.htm#clean_bus

Nylund, N.-O.; Erkkilä, K.; Lappi, M.; Ikonen, M. (2004). Transit Bus Emission Study: Comparison of Emissions from Diesel and Natural Gas Buses; VTT Technical Research Centre of Finland; Research Report. Project 3/P5150/04. 2004.

PLANYC 2030. Air Quality. Available at: http://www.nyc.gov/html/planyc2030/downloads/pdf/report_air_quality.pdf

Prucz, J. C.; Clark, N. N.; Gautam, M.; Lyons, D. W. Exhaust emissions from engines of the Detroit Diesel Corporation in transit buses: A decade of trends. *Environ. Sci. Technol*. **2001**, *35*, 1755-1764.

Ristovski, Z. D.; Jayaratne, E. R.; Lim, M.; Ayoko, G. A.; Morawska, L. Influence of diesel fuel sulfur on nanoparticle emissions from city buses. *Environ. Sci. Technol*. **2006**, *40*, 1314-1320.

Robert, M. A.; Kleeman, M. J.; Jakober, C. A. Size and composition distributions of particulate matter emissions: Part 2—Heavy-duty diesel vehicles. *J. Air & Waste Manage. Assoc.* **2007**, *57*, 1429-1438.

Rönkkö, T.; Virtanen, A.; Vaaraslahti, K.; Keskinen, J.; Pirjola, L.; Lappi, M. Effect of dilution conditions and driving parameters on nucleation mode particles in diesel exhaust: Laboratory and on-road study. *Atmospheric Environment*. **2006**, *40* (16), 2893-2901.

Shi, J. P.; Mark, D.; Harrison, R. M. Characterization of particles from a current technology heavy-duty diesel engine. *Environ. Sci. Technol*. **2000**, *34*, 748-755.

Sioutas, C.; Delfino, J.; Singh, M. Exposure assessment for atmospheric ultrafine particles and implications in epidemiologic research. *Environmental Health Perspectives.* **2005**, *113*, 947-955.

Sonntag, D.B., H. O. Gao, and B. A. Holmén. Variability of particle number emissions from diesel and hybrid diesel-electric buses in real driving conditions. *Environ. Sci. & Technol*. **2008**, 42, 5637-5643.

Vaaraslahti, K.; Virtanen, A.; Ristimäki, J.; Keskinen, J. Nucleation mode formation in heavy-duty diesel exhaust with and without a particulate filter. *Environ. Sci. Technol*. **2004**, *38* (18), 4884-4890.

Vikara, D.; Holmen, B. A. Ultrafine particle number concentrations from hybrid urban transit buses: Onboard single-diameter Scanning Mobility Particle Sizer Measurements. *Transportation Research Record*. **2006**, *1987*, 54 -61.

Wichmann, H. E.; Peters, A.; Epidemiological evidence of the effects of ultrafine particle exposure. In *Ultrafine Particles in the Atmosphere*; Brown, L. M., Collings, N., Harrison, R. M., Maynard, A.D., Maynard, R.L., Eds.; Imperial College Press: London, 2000.

Zhang K. M.; Wexler, A. S.; Niemeier, D. A.; Zhu Y. F.; Hinds, W. C.; Sioutas, C. Evolution of particle number distributions near roadways Part III: Traffic analysis and on-road size resolved particulate emission factors. *Atmospheric Environment*. **2005**, *39*(22), 4155-4166.

Zhu, Y.; Hinds, W.; Kim, S.; Sioutas, C. Concentration and size distribution of ultrafine particles near a major highway. *J. Air Waste Manage. Assoc*. **2002**, *52*, 1032–1042.